


## Queueing theory of search processes with stochastic resetting

Paul C. Bressloff *Department of Mathematics, University of Utah, Salt Lake City, Utah 84112, USA* (Received 25 April 2020; revised 5 July 2020; accepted 21 August 2020; published 8 September 2020)

We use queueing theory to develop a general framework for analyzing search processes with stochastic resetting, under the additional assumption that following absorption by a target, the particle (searcher) delivers a packet of resources to the target and the search process restarts at the reset point  $\mathbf{x}_r$ . This leads to a sequence of search-and-capture events, whereby resources accumulate in the target under the combined effects of resource supply and degradation. Combining the theory of  $G/M/\infty$  queues with a renewal method for analyzing resetting processes, we derive general expressions for the mean and variance of the number of resource packets within the target at steady state. These expressions apply to both exponential and nonexponential resetting protocols and take into account delays arising from various factors such as finite return times, refractory periods, and delays due to the loading or unloading of resources. In the case of exponential resetting, we show how the resource statistics can be expressed in terms of the MFPTs  $T_r(\mathbf{x}_r)$  and  $T_{r+\gamma}(\mathbf{x}_r)$ , where  $r$  is the resetting rate and  $\gamma$  is the degradation rate. This allows us to derive various general results concerning the dependence of the mean and variance on the parameters  $r$ ,  $\gamma$ . Our results are illustrated using several specific examples. Finally, we show how fluctuations can be reduced either by allowing the delivery of multiple packets that degrade independently or by having multiple independent searchers.

DOI: [10.1103/PhysRevE.102.032109](https://doi.org/10.1103/PhysRevE.102.032109)

### I. INTRODUCTION

A topic of considerable current interest concerns search processes with stochastic resetting (see the review in Ref. [1]). One major motivating example is a diffusing particle searching for a hidden target in an unbounded domain. The introduction of stochastic resetting, whereby the position of the searcher is reset to a fixed location  $\mathbf{x}_r \in \mathbb{R}^d$  at a rate  $r$ , renders the mean first passage time (MFPT) finite. Moreover, there exists an optimal resetting rate at which the MFPT is minimized [2–4]. Similar behavior has been observed in a variety of other stochastic search processes with resetting, including nondiffusive processes such as Levy flights [5] and velocity jump processes [6–8], drift-diffusion processes [9], and resetting in a potential landscape [10,11] or in bounded domains [12,13]. Other recent extensions include the incorporation of delays such as finite return times and refractory periods [14–19], and the introduction of nonexponential resetting protocols [20–22]. Several authors have focused on extracting universal features of search processes with resetting, deriving general expressions for MFPTs and other statistical quantities that include the effects of delays, nonexponential resetting rates, and multiple targets [23–29].

A common assumption of these and related studies is that once the searcher has found the target, it is absorbed and the search process ends. However, there are a number of examples in cell biology where the arrival of a particle results in the delivery of some resource to the target, after which the particle escapes and returns to its initial position. The particle may then be resupplied with cargo and initiate a new search process. Two examples are as follows: (i) the motor-driven

intracellular transport of vesicles to synaptic targets in the axons and dendrites of neurons [30–32] and (ii) the transport of morphogen at the tips of growing actin-rich filaments (cytonemes) to target cells during embryonic development in vertebrates [33–36]. In the first example the particle (searcher) represents a molecular motor complex moving along a polymerized filament such as a microtubule within the axon or dendrite of a neuron, while resetting corresponds to the removal and return of the complex to the cell body. In the second example, the particle represents the tip of a growing cytoneme, while resetting takes into account the fact that a cytoneme can switch to a shrinkage phase and rapidly retract back to the source cell, see Fig. 1. In both of these applications, the restart of the search process following reset has a finite duration with two components: a finite return time and a refractory period. The return time could depend on the speed of retrograde motor transport or the rate of cytoneme retraction, while the refractory period could depend on the time to reload a motor complex with vesicles at the cell body or the time for a new cytoneme to nucleate from the source cell. Previously we have used velocity jump processes to model both motor-driven [37–39] and cytoneme-based [19,40] transport. In the latter case we showed how queueing theory can be used to analyze the accumulation of morphogen in a one-dimensional (1D) array of target cells following multiple rounds of search-and-capture, analogously to studies of gene transcription [41].

In this paper we use queueing theory to develop a general framework for analyzing search processes with stochastic resetting, under the additional assumption that following absorption by a target, the particle delivers a packet of resources to the target, after which it returns to the reset position  $\mathbf{x}_r$ . This

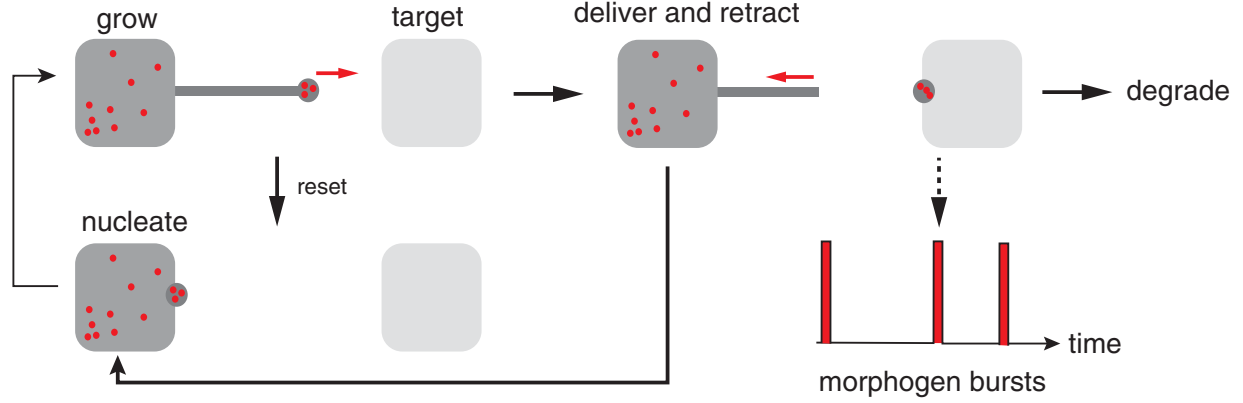


FIG. 1. Multiple search-and-capture events for cytoneme-based morphogen transport. Alternating periods of growth, shrinkage, nucleation, and target capture generate a sequence of morphogen bursts in a given target cell. This results in the accumulation of morphogen within the cell, which is balanced by degradation.

leads to a sequence of search-and-capture events, whereby resources accumulate in the target. We also assume that the build up of resources within the target is counterbalanced by degradation, so that there is a steady-state number of packets in the long-time limit. Queuing theory concerns the mathematical analysis of waiting lines formed by customers randomly arriving at some service station, and staying in the system until they receive service from a group of servers [42,43]. A sequence of search-and-capture events can be mapped onto a queuing process as follows: Individual resource packets are analogous to customers, the delivery of a packet corresponds to a customer arriving at the service station, and the degradation of a resource packet is the analog of a customer exiting the system after being serviced. Finally, assuming that the packets are degraded independently of each other, the effective number of servers in the corresponding queuing model is infinite, that is, the presence of other customers does not affect the service time of an individual customer. It follows that the relevant queuing model is the  $G/M/\infty$  system [42,43]. Here the symbol  $G$  denotes a general customer interarrival time distribution  $F(t)$ , the symbol  $M$  stands for a Markovian or exponential service-time distribution  $\Phi(t) = 1 - e^{-\gamma t}$ , and “ $\infty$ ” denotes infinite servers. In terms of a search process with stochastic resetting, we identify  $F(t)$  with the cumulative first passage time (FPT) distribution. That is,  $F(t) = \int_0^t f_r(\mathbf{x}_r, t') dt'$ , where  $f_r(\mathbf{x}_r, t)$  is the FPT density for the particle to find the target starting from  $\mathbf{x}_r$ . The latter can itself be expressed in terms of the FPT without resetting,  $f_0(\mathbf{x}_r, t)$ , using renewal theory. Similarly, we identify  $-\Phi'(t)$  with the waiting time density for degradation at a rate  $\gamma$ .

The main goal of this paper is to derive general expressions for the mean and variance of the number of resource packets within the target at steady-state in the case of a search process with resetting. We begin by considering multiple search-and-capture events for a search process in some domain  $\mathcal{U} \subseteq \mathbb{R}^d$  with a single target  $\mathcal{U}_0 \subset \mathcal{U}$  (Sec. II). The search process is taken to evolve according to a master equation without resetting. We formulate the accumulation of resources in terms of a  $G/M/\infty$  queue [42,43] and derive an iterative integral equation for the binomial moments of the number  $N(t)$  of packets in the target at time  $t$ . The integral equation is solved

using Laplace transforms, which is then used to obtain explicit expressions for the mean and variance of  $N(t)$  in the steady state; these depend on the Laplace transform  $\tilde{f}_0(\mathbf{x}_0, s)$  of the FPT density for a single search-and-capture event starting from  $\mathbf{x}_0$ . In Sec. III we consider a single search-and-capture event with stochastic resetting. We derive a general expression for the corresponding FPT density in Laplace space,  $\tilde{f}_r(\mathbf{x}_r, s)$ , using a renewal method that has been developed by a number of authors, see for example Refs. [24–26,28,29]. The renewal method exploits the fact that once the particle has returned to  $\mathbf{x}_r$  it has lost all memory of previous search phases. It follows that one can condition on whether or not the particle resets at least once, even though a reset event occurs at random times. Note that a similar approach has also been applied to other types of FPT problems, including the narrow escape from a domain with stochastically gated boundaries [38,44] and cytoneme-based morphogen transport [19,40].

In Sec. IV we combine the analysis presented in Secs. II and Sec. III to analyze multiple search-and-capture events in the presence of resetting. We focus on the case of exponential resetting without delays and show how the resource statistics can be expressed in terms of the MFPTs  $T_r(\mathbf{x}_r)$  and  $T_{r+\gamma}(\mathbf{x}_r)$ , where  $r$  is the resetting rate and  $\gamma$  is the degradation rate. This allows us to derive various general results concerning the dependence of the mean  $\bar{N}$  and variance  $\text{Var}[N]$  on the parameters  $r, \gamma$ . The theory is then illustrated in Sec. V by considering several examples of search processes, including diffusion on the half-line and finite interval, a 1D velocity jump process, and diffusive search for a spherical target. Outside the slow resetting regime, we find that the Fano factor  $\text{Var}[N]/\bar{N}$  lies in a neighborhood of unity so that the mean and variance are comparable (Poisson-like noise). In such cases, the corresponding coefficient of variance (CV) varies as  $1/\sqrt{\bar{N}}$  and is thus much more sensitive to parameter variations. Finally, in Sec. VI we generalize the analysis of the binomial moments to allow for the simultaneous delivery of multiple packets that degrade independently. This leads to a reduction in the CV. We also show that a more effective way to reduce fluctuations is to have multiple searchers transporting a single packet.

## II. MULTIPLE SEARCH-AND-CAPTURE EVENTS AND QUEUEING THEORY

Consider a particle (searcher) subject to stochastic motion in  $\mathcal{U} \subseteq \mathbb{R}^d$ . Suppose that there exists some target  $\mathcal{U}_0 \subset \mathbb{R}^d$  whose boundary  $\partial\mathcal{U}_0$  is absorbing and  $\mathbf{x}_r \notin \mathcal{U}_0$ . The probability density  $p(\mathbf{x}, t|\mathbf{x}_0)$  for the particle to be at position  $\mathbf{x}$  at time  $t$ , having started at  $\mathbf{x}_0$ , is taken to evolve according to the master equation

$$\frac{\partial p(\mathbf{x}, t|\mathbf{x}_0)}{\partial t} = \mathbb{L}p(\mathbf{x}, t|\mathbf{x}_0), \quad (2.1)$$

where  $\mathbb{L}$  is the infinitesimal generator of the stochastic process. This is supplemented by the absorbing boundary condition  $p(\mathbf{x}, t|\mathbf{x}_0) = 0$  for all  $\mathbf{x} \in \partial\mathcal{U}_0$  and the reflecting boundary condition  $\partial_n p(\mathbf{x}, t|\mathbf{x}_0) = 0$  for all  $\mathbf{x} \in \partial\mathcal{U}$ . (In the case of unbounded domains, the latter is replaced by the far-field condition  $p(\mathbf{x}, t|\mathbf{x}_0) \rightarrow 0$  as  $|\mathbf{x}| \rightarrow \infty$ .) Let  $\mathcal{T}(\mathbf{x}_0)$  denote the FPT to be absorbed by the target, having started at  $\mathbf{x}_0$ :

$$\mathcal{T}(\mathbf{x}_0) = \inf\{t > 0; \mathbf{X}(t) \in \partial\mathcal{U}_0, \mathbf{X}(0) = \mathbf{x}_0\}. \quad (2.2)$$

The MFPT can be expressed in terms of a survival probability according to

$$T_0(\mathbf{x}_0) = \mathbb{E}[\mathcal{T}(\mathbf{x}_0)] = \int_0^\infty Q_0(\mathbf{x}_0, t)dt, \quad (2.3)$$

where

$$Q_0(\mathbf{x}_0, t) = \int_{\mathcal{U} \setminus \mathcal{U}_0} p(\mathbf{x}, t|\mathbf{x}_0)d\mathbf{x}. \quad (2.4)$$

Now suppose that rather than being permanently absorbed or captured by the target, the particle delivers a discrete packet of some resource and then returns to  $\mathbf{x}_0$ , initiating another round of search-and-capture. (The return to  $\mathbf{x}_0$  is distinct from resetting, which can occur at any time, see Sec. III.) We will refer to the delivery of a single packet as a burst event. The sequence of bursts resulting from multiple rounds of search-and-capture leads to an accumulation of packets within the target, which we assume is counteracted by degradation at some rate  $\gamma$ . This is illustrated in Fig. 2 for a target in a rectangular domain. We will assume that the total time for the particle to unload its cargo, return to  $\mathbf{x}_0$ , and start a new search process is given by the random variable  $\hat{\tau}$ , which for simplicity is taken to be independent of the location of the targets. (This is reasonable if the sum of the mean loading and unloading times is much larger than a typical return time.) Let  $n \geq 1$  label the  $n$ th burst event. If  $\tau_n$  is the time of the  $n$ th burst, then the interarrival times are

$$\Delta_n := \tau_n - \tau_{n-1} = \hat{\tau}_n + \mathcal{T}(\mathbf{x}_0), \quad n \geq 1. \quad (2.5)$$

Denoting the waiting time density of the delays  $\hat{\tau}_n$  by  $\rho(\hat{\tau})$ , the interarrival time density is given by

$$\begin{aligned} \mathcal{F}(\Delta) &= \int_0^\Delta dt \int_0^\Delta d\hat{\tau} \delta(\Delta - t - \hat{\tau}) f_0(t) \rho(\hat{\tau}) \\ &= \int_0^\Delta f_0(t) \rho(t - \Delta) dt, \end{aligned} \quad (2.6)$$

where  $f_0(t) = -dQ_0/dt$  is the FPT density for a single search-and-capture event that delivers a packet to the target.

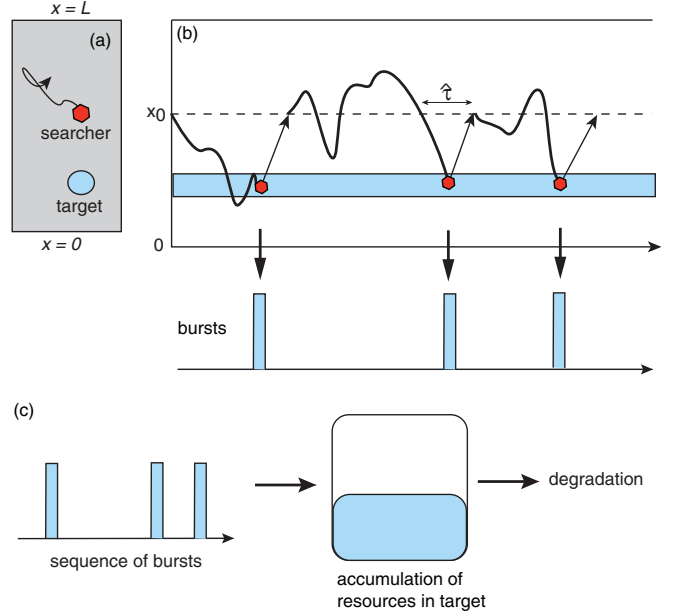


FIG. 2. Multiple search-and-capture events. (a) Particle searching in a rectangular domain with a single target. Each time the particle reaches the target it delivers a discrete packet of resources (burst event) and then returns to  $\mathbf{x}_0$  where it is loaded with another packet and the process repeats. (b) Sample trajectory projected onto the  $x$  coordinate showing a sequence of burst events. The delay time  $\hat{\tau}$  between a burst event and initiation of a new search is generated from a waiting time density  $\rho(\hat{\tau})$ . (The lines with arrows do not represent actual trajectories.) (c) The burst sequence results in an accumulation of resource packets within the target, which is counteracted by degradation at some rate  $\gamma$ .

(For notational simplicity, we have dropped the explicit dependence on the initial position  $\mathbf{x}_0$ .) Laplace transforming the convolution equation then yields

$$\tilde{\mathcal{F}}(s) = \tilde{f}_0(s) \tilde{\rho}(s). \quad (2.7)$$

As highlighted in the Introduction, multiple search-and-capture events can be mapped onto a  $G/M/\infty$  queuing process, in which individual resource packets are analogous to customers. Each burst event corresponds to a customer arriving at the service station according to an interarrival distribution  $F(t)$ , and the degradation of a resource packet at a rate  $\gamma$  is the analog of a customer exiting the system after being serviced via an exponential service-time distribution, with  $\Phi(t) = 1 - e^{-\gamma t}$  the probability that degradation occurs after time  $t$ . Since the packets are degraded independently of each other, the effective number of servers in the corresponding queuing model is infinite, that is, the presence of other customers does not affect the service time of an individual customer. Finally, the distribution  $F(t)$  is related to the interarrival time density  $\mathcal{F}(t)$  of a single search-and-capture event according to

$$F(t) = \int_0^t \mathcal{F}(y) dy. \quad (2.8)$$

We will use classical queuing theory to determine the steady-state statistics of resource accumulation within the target. For further details see Refs. [42,43].

Let  $N(t)$  be the number of busy servers at time  $t$ . This corresponds to the number of packets in the target that have not yet degraded. In terms of the sequence of arrival times  $\tau_n$ , we can write

$$N(t) = \sum_{n, 0 \leq \tau_n \leq t} I(t - \tau_n, S_n), \quad (2.9)$$

where

$$I(t - \tau_n, S_n) = \begin{cases} 1 & \text{if } t - \tau_n \leq S_n \\ 0 & \text{if } t - \tau_n > S_n \end{cases}. \quad (2.10)$$

Here  $S_n$  is the service (degradation) time of the  $n$ th packet. Introduce the generating function

$$G(z, t) = \sum_{l=0}^{\infty} z^l \mathbb{P}[N(t) = l], \quad (2.11)$$

and the binomial moments

$$B_m(t) = \sum_{l=m}^{\infty} \frac{l!}{(l-m)!m!} \mathbb{P}[N(t) = l], \quad m = 1, 2, \dots \quad (2.12)$$

Suppose that the target is empty at time  $t = 0$ . We derive an integral equation for the generating function  $G(z, t)$ . Conditioning the first arrival time by setting  $\tau_1 = y$ , we have

$$N(t) = \begin{cases} I(t - y, S_1) + N^*(t - y) & \text{if } y \leq t \\ 0 & \text{if } y > t \end{cases}, \quad (2.13)$$

where  $N^*(t)$  has the same distribution as  $N(t)$ . Note that  $I(t - y, S_1)$  and  $N^*(t - y)$  are independent. Moreover,

$$\mathbb{P}[I(t - y, S_1) = j] = [1 - \Phi(t - y)]\delta_{j,1} + \Phi(t - y)\delta_{j,0}, \quad (2.14)$$

so it follows that

$$\sum_{j=0,1} z^j \mathbb{P}[I(t - y, S_1) = j] = z + (1 - z)\Phi(t - y). \quad (2.15)$$

The total expectation theorem yields

$$\begin{aligned} \mathbb{E}[z^{I(t-\tau_1, S_1)}] &= \mathbb{E}[\mathbb{E}[z^{I(t-\tau_1, S_1)} | \tau_1 = y]] \\ &= \int_0^{\infty} [z + (1 - z)\Phi(t - y)] dF(y). \end{aligned} \quad (2.16)$$

Another application of the total expectation theorem gives

$$\begin{aligned} G(z, t) &= \mathbb{E}[z^{N(t)}] = \mathbb{E}[\mathbb{E}[z^{N(t)} | \tau_1 = y]], \\ &= \int_t^{\infty} dF(y) + \int_0^t [z + (1 - z)\Phi(t - y)] G(z, t - y) dF(y). \end{aligned} \quad (2.18)$$

Differentiating Eq. (2.18) with respect to  $z$  and using

$$B_m(t) = \frac{1}{m!} \left. \frac{d^m G(z, t)}{dz^m} \right|_{z=1} \quad (2.19)$$

leads to an iterative integral equation for the binomial moments:

$$\begin{aligned} B_m(t) &= \int_0^t B_m(t - y) dF(y) \\ &+ \int_0^t B_{m-1}(t - y) [1 - \Phi(t - y)] dF(y). \end{aligned} \quad (2.20)$$

In order to obtain the steady-state binomial moments, we Laplace transform Eq. (2.20) after setting  $dF(y) = \mathcal{F}(y)dy$  and  $1 - \Phi(t - y) = e^{-\gamma(t-y)}$ :

$$\tilde{B}_m(s) = \left[ \frac{\tilde{\mathcal{F}}(s)}{1 - \tilde{\mathcal{F}}(s)} \right] \tilde{B}_{m-1}(s + \gamma). \quad (2.21)$$

Multiplying both sides by  $s$  and taking the limit  $s \rightarrow 0^+$  yields

$$B_m^* = \lim_{t \rightarrow \infty} B_m(t) = \lim_{s \rightarrow 0^+} s \tilde{B}_m(s) = \lambda \tilde{B}_{m-1}(\gamma), \quad (2.22)$$

where

$$\lambda := \lim_{s \rightarrow 0^+} \frac{s \tilde{\mathcal{F}}(s)}{1 - \tilde{\mathcal{F}}(s)} = \frac{1}{T_0 + \langle \hat{\tau} \rangle}. \quad (2.23)$$

We have used L'Hopital's rule and Eq. (2.7) together with the following properties:

$$\tilde{f}_0(0) = 1 = \tilde{\rho}(0), \quad \left. \frac{d\tilde{f}_0}{ds} \right|_{s=0} = -T_0, \quad \left. \frac{d\tilde{\rho}}{ds} \right|_{s=0} = -\tau_{\text{cap}}. \quad (2.24)$$

Here  $\tau_{\text{cap}}$  is the mean time for loading and unloading a packet. Equations (2.21) and (2.22) completely determine the steady-state binomial moments. In particular, since  $B_0(t) = 1$  and  $\tilde{B}_0(s) = 1/s$ , the mean number of packets in the target is

$$B_1^* \equiv \bar{N} = \frac{\lambda}{\gamma} = \frac{1}{\gamma(T_0 + \tau_{\text{cap}})}. \quad (2.25)$$

We can thus interpret  $\lambda$  as the mean rate at which a packet is delivered to the target. This is consistent with Eq. (2.22), since  $T_0 + \tau_{\text{cap}}$  is the mean time for one successful delivery of a packet and initiation of a new round of search-and-capture. Hence, its inverse is the mean rate of resource bursts. Note that this result is quite general and is known as Little's law in the queuing theory literature [45].

The above analysis can also be used to determine the higher-order statistics of the resource distribution. For example,

$$B_2^* \equiv \frac{1}{2} (\langle N^2 \rangle - \bar{N}) = \lambda \tilde{B}_1(\gamma) = \frac{\lambda}{2\gamma} \frac{\tilde{\mathcal{F}}(\gamma)}{1 - \tilde{\mathcal{F}}(\gamma)}. \quad (2.26)$$

Hence, the variance of the number of resource packets is

$$\begin{aligned} \text{Var}[N] &= 2B_2^* + B_1^*(1 - B_1^*) \\ &= \frac{\lambda}{\gamma} \left[ \frac{\tilde{\mathcal{F}}(\gamma)}{1 - \tilde{\mathcal{F}}(\gamma)} + 1 - \frac{\lambda}{\gamma} \right]. \end{aligned} \quad (2.27)$$

It can be seen that although the mean  $\bar{N}$  only depends on the mean  $T_0$ , higher-order moments involve the Laplace transform of the FPT densities  $f_0(t)$ .

### III. SINGLE SEARCH-AND-CAPTURE EVENT WITH STOCHASTIC RESETTING

Now suppose that prior to being absorbed by the target, the particle can reset to a fixed location  $\mathbf{x}_r$  at a random sequence of times generated by a probability density  $\psi(\tau)$ , see Fig. 3. It follows that  $\Psi(\tau) = 1 - \int_0^\tau \psi(s) ds$  is the probability that no resetting has occurred up to time  $\tau$ . (In the following we also take  $\mathbf{x}_0 = \mathbf{x}_r$ .) Rather than instantaneously returning to  $\mathbf{x}_r$ , we assume that the particle switches to a ballistic state in which it

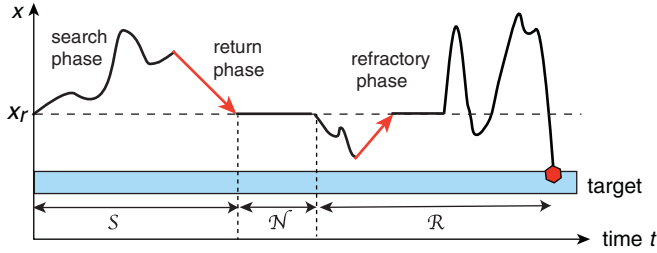


FIG. 3. Single search-and-capture event with resetting. Particle searching for a target that is found after two resettings. Following each resetting event, the particle returns to the point  $x_r$  at a constant speed  $V$ , after which it remains at  $x_r$  for a refractory period before re-entering the search phase. Also shown is the decomposition of the FPT,  $\mathcal{T} = S + \mathcal{N} + \mathcal{R}$ .

returns to  $\mathbf{x}_r$  at a constant speed  $V$ . (For simplicity, the particle cannot be absorbed by the target when it is in the return phase. One could also consider a more general dynamical model for the return phase as in Refs. [18,28].) In addition, whenever the particle returns to  $\mathbf{x}_r$ , it is subject to a refractory period before the search begins again. The refractory period is itself a random variable with a corresponding waiting time density  $\phi$ , which is taken to have a finite mean  $\tau_{\text{ref}}$ . We want to determine the FPT density to be absorbed by the target in the presence of resetting with delays (a single search-and-capture event with resetting). A number of authors have studied the general FPT problem for stochastic processes with resetting using renewal theory, which exploits the fact that once the particle has returned to  $\mathbf{x}_r$  it has lost all memory of previous search phases [23–29]. (An analogous scenario occurs in cytoneme-based morphogenesis [19,40].) This means that one can condition on whether or not the particle resets at least once, even though a reset event occurs at random times. Renewal theory can take into account delays and nonexponential resetting, as well as non-Markovian search processes that cannot be modeled in terms of a master equation. Here we consider a formulation of renewal theory [29] that is equivalent to the analysis of Ref. [28] in the case of search processes generated by the master equation (2.1).

Let  $\mathcal{I}(t)$  denote the number of resets that have occurred up to time  $t$ . Consider the following set of FPTs, corresponding to the decompositions shown in Fig. 3:

$$\begin{aligned} \mathcal{T} &= \inf\{t > 0; \mathbf{X}(t) \in \partial\mathcal{U}_0, \mathcal{I}(t) \geq 0\}, \\ \mathcal{S} &= \inf\{t > 0; \mathbf{X}(t) = \mathbf{x}_r, \mathcal{I}(t) = 1\}, \\ \mathcal{R} &= \inf\{t > 0; \mathbf{X}(t + \mathcal{S} + \mathcal{N}) \in \partial\mathcal{U}_0, \mathcal{I}(t + \mathcal{S} + \mathcal{N}) \geq 1\}. \end{aligned} \quad (3.1)$$

Here  $\mathcal{T}$  is the FPT for finding the target irrespective of the number of resettings,  $\mathcal{S}$  is the FPT for the first resetting and return to the reset point  $\mathbf{x}_r$  given that the particle is still free,  $\mathcal{N}$  is the first refractory time, and  $\mathcal{R}$  is the FPT for finding the target given that at least one resetting has occurred. Next we introduce the sets  $\Omega = \{\mathcal{T} < \infty\}$  and  $\Gamma = \{\mathcal{S} < \mathcal{T} < \infty\} \subset \Omega$ . Here  $\Omega$  is the set of all events for which the particle is eventually absorbed by the target (which has measure one), and  $\Gamma$  is the subset of events in  $\Omega$  for which the particle resets at least once. It immediately follows that  $\Omega \setminus \Gamma = \{\mathcal{T} < \mathcal{S} = \infty\}$ , that is,  $\Omega \setminus \Gamma$  is the set of all events for which the particle is captured by the target without any resetting.

The Laplace transform of the FPT density with resetting is

$$\tilde{f}_r(\mathbf{x}_r, s) = \mathbb{E}[e^{-s\mathcal{T}} 1_{\Omega}]. \quad (3.2)$$

Following along the lines of Refs. [28,29], consider the decomposition

$$\mathbb{E}[e^{-s\mathcal{T}} 1_{\Omega}] = \mathbb{E}[e^{-s\mathcal{T}} 1_{\Omega \setminus \Gamma}] + \mathbb{E}[e^{-s\mathcal{T}} 1_{\Gamma}]. \quad (3.3)$$

The first expectation can be evaluated by noting that it is the FPT density for capture by the target without any resetting, and the probability density for such an event is  $-\Psi(t) \partial_t Q_0(\mathbf{x}_r, t) dt$ , where  $Q_0$  is the survival probability (2.4). Hence,

$$\begin{aligned} \mathbb{E}[e^{-s\mathcal{T}} 1_{\Omega \setminus \Gamma}] &= - \int_0^{\infty} e^{-s\tau} \Psi(\tau) \frac{\partial Q_0(\mathbf{x}_r, \tau)}{\partial \tau} d\tau \\ &= 1 - \int_0^{\infty} e^{-s\tau} \psi(\tau) Q_0(\mathbf{x}_r, \tau) d\tau - s \\ &\quad \times \int_0^{\infty} e^{-s\tau} \Psi(\tau) Q_0(\mathbf{x}_r, \tau) d\tau. \end{aligned} \quad (3.4)$$

The second expectation can be written as

$$\begin{aligned} \mathbb{E}[e^{-s\mathcal{T}} 1_{\Gamma}] &= \mathbb{E}[e^{-s(\mathcal{S} + \mathcal{N} + \mathcal{R})} 1_{\Gamma}] \\ &= \int_0^{\infty} \psi(\tau_1) \left[ \int_{\mathcal{U} \setminus \mathcal{U}_0} e^{-s(\tau_1 + |\mathbf{x} - \mathbf{x}_r|/V)} p(\mathbf{x}, \tau_1 | \mathbf{x}_r) d\mathbf{x} \right] \\ &\quad \times d\tau_1 \left[ \int_0^{\infty} e^{-s\tau_2} \phi(\tau_2) d\tau_2 \right] \tilde{f}_r(\mathbf{x}_r, s). \end{aligned} \quad (3.5)$$

We have used the fact that the probability that the first return is initiated in the interval  $[\tau_1, \tau_1 + d\tau_1]$ , given that  $\mathbf{X}(\tau_1) = \mathbf{x}$  and the particle has not been captured by the target, is  $\psi(\tau_1) p(\mathbf{x}, \tau_1 | \mathbf{x}_r) d\tau_1$ . The particle then takes an additional time  $|\mathbf{x} - \mathbf{x}_r|/V$  to return to  $\mathbf{x}_r$ , after which it spends a time  $\tau_2$  in the refractory state with waiting time density  $\phi(\tau_2)$ . The remaining time to find the target has the same FPT density as  $\mathcal{T}$ . Combining Eqs. (3.3)–(3.5) and rearranging yields the general result [28]

$$\tilde{f}_r(\mathbf{x}_r, s) = \frac{1 - \int_0^{\infty} e^{-s\tau} \psi(\tau) Q_0(\mathbf{x}_r, \tau) d\tau - s \int_0^{\infty} e^{-s\tau} \Psi(\tau) Q_0(\mathbf{x}_r, \tau) d\tau}{1 - \tilde{\phi}_{\text{ref}}(s) \int_0^{\infty} \psi(\tau_1) \left[ \int_{\mathcal{U} \setminus \mathcal{U}_0} e^{-s(\tau_1 + |\mathbf{x} - \mathbf{x}_r|/V)} p(\mathbf{x}, \tau_1 | \mathbf{x}_r) d\mathbf{x} \right] d\tau_1}. \quad (3.6)$$

The Laplace transform of the FPT density is the moment generator of the FPT  $\mathcal{T}$ :

$$T_r^{(n)} = \mathbb{E}[\mathcal{T}^n 1_{\Omega}] = \left( -\frac{d}{ds} \right)^n \mathbb{E}[e^{-s\mathcal{T}} 1_{\Omega}] \Big|_{s=0}. \quad (3.7)$$

For example, the MFPT  $T_r = T_r^{(1)}$  is

$$\begin{aligned} T_r(\mathbf{x}_r) &= \frac{\langle Q_0(\mathbf{x}_r, \tau) \rangle_\psi - \langle \tau Q_0(\mathbf{x}_r, \tau) \rangle_\psi}{1 - \langle Q_0(\mathbf{x}_r, \tau) \rangle_\psi} + \frac{-\tilde{\phi}'_{\text{ref}}(0) \langle Q_0(\mathbf{x}_r, \tau) \rangle_\psi + \langle \tau Q_0(\mathbf{x}_r, \tau) \rangle_\psi + V^{-1} \langle F(\mathbf{x}_r, \tau) \rangle_\psi}{1 - \langle Q_0(\mathbf{x}_r, \tau) \rangle_\psi} \\ &= \frac{\langle Q_0(\mathbf{x}_r, \tau) \rangle_\psi + \tau_{\text{ref}} \langle Q_0(\mathbf{x}_r, \tau) \rangle_\psi + V^{-1} \langle F(\mathbf{x}_r, \tau) \rangle_\psi}{1 - \langle Q_0(\mathbf{x}_r, \tau) \rangle_\psi}, \end{aligned} \quad (3.8)$$

where we have set

$$\langle Q_0(\mathbf{x}_r, \tau) \rangle_\psi = \int_0^\infty \psi(\tau) Q_0(\mathbf{x}_r, \tau) d\tau, \quad (3.9)$$

etc., and

$$F(\mathbf{x}_r, t) = \int_{\mathcal{U} \setminus \mathcal{U}_0} |\mathbf{x} - \mathbf{x}_r| p(\mathbf{x}, t | \mathbf{x}_r) d\mathbf{x}. \quad (3.10)$$

We have also used the result

$$-\tilde{\phi}'_{\text{ref}}(0) = \tau_{\text{ref}} = \int_0^\infty \tau \phi(\tau) d\tau. \quad (3.11)$$

In the case of exponential resetting,

$$\psi(t) = r e^{-rt}, \quad \Psi(\tau) = e^{-r\tau}, \quad (3.12)$$

everything can be expressed in terms of Laplace transforms. For example, the MFPT reduces to

$$T_r(\mathbf{x}_r) = \frac{\tilde{Q}_0(\mathbf{x}_r, r) + r \tau_{\text{ref}} \tilde{Q}_0(\mathbf{x}_r, r) + r \tilde{F}(\mathbf{x}_r, r)/V}{1 - r \tilde{Q}_0(\mathbf{x}_r, r)}, \quad (3.13)$$

where  $\tilde{F}(\mathbf{x}_r, r)$  is the Laplace transform of  $F(\mathbf{x}_r, \tau)$ . Similarly, the Laplace transform of the FPT density becomes

$$\tilde{f}_r(\mathbf{x}_r, s) = \frac{1 - (r+s) \tilde{Q}_0(\mathbf{x}_r, r+s)}{1 - r \tilde{\phi}(s) \int_{\mathcal{U} \setminus \mathcal{U}_0} e^{-s|\mathbf{x} - \mathbf{x}_r|/V} \tilde{p}(\mathbf{x}, r+s | \mathbf{x}_r) d\mathbf{x}}. \quad (3.14)$$

#### IV. MULTIPLE SEARCH-AND-CAPTURE EVENTS WITH RESETTING

We can now combine the results of Secs. II and III to analyze the accumulation of resources in a target due to multiple rounds of search-and-capture events with resetting. This is achieved by setting  $\tilde{\mathcal{F}}(s) = f_r(\mathbf{x}_r, s) \tilde{\rho}(s)$ , see Eq. (2.7). In order to develop our intuition, we mainly focus on the case of exponential resetting and no delays. However, the theory developed in this paper applies to a much more general class of search processes, which we hope to explore more fully elsewhere.

##### A. Instantaneous resetting

Suppose that  $\phi(\tau) = \rho(\tau) = \delta(\tau)$  and take the limit  $V \rightarrow \infty$ . Equations (3.13) and (3.14) then become

$$T_r(\mathbf{x}_r) = \frac{\tilde{Q}_0(\mathbf{x}_r, r)}{1 - r \tilde{Q}_0(\mathbf{x}_r, r)}, \quad (4.1)$$

and

$$\tilde{f}_r(\mathbf{x}_r, s) = \frac{1 - (r+s) \tilde{Q}_0(\mathbf{x}_r, r+s)}{1 - r \tilde{Q}_0(\mathbf{x}_r, r+s)}. \quad (4.2)$$

In terms of the FPT density  $f_0$  without resetting, whose Laplace transform is

$$\tilde{f}_0(\mathbf{x}_r, s) = 1 - s \tilde{Q}_0(\mathbf{x}_r, s), \quad (4.3)$$

we can write

$$T_r(\mathbf{x}_r) = \frac{1 - \tilde{f}_0(\mathbf{x}_r, r)}{r \tilde{f}_0(\mathbf{x}_r, r)}, \quad (4.4)$$

and

$$\tilde{f}_r(\mathbf{x}_r, s) = \frac{(r+s) \tilde{f}_0(\mathbf{x}_r, r+s)}{s + r \tilde{f}_0(\mathbf{x}_r, r+s)}. \quad (4.5)$$

This recovers the more general result derived in Ref. [24].

Substituting Eq. (4.5) into Eqs. (2.21) and (2.22) with  $\tilde{\mathcal{F}}(s) = f_r(\mathbf{x}_r, s)$  yields the following iterative equation for the binomial moments:

$$\begin{aligned} \tilde{B}_m(\gamma) &= \frac{r+\gamma}{\gamma} \frac{\tilde{f}_0(\mathbf{x}_r, r+\gamma)}{1 - \tilde{f}_0(\mathbf{x}_r, r+\gamma)} \tilde{B}_{m-1}(2\gamma) \\ &= \frac{1}{\gamma T_{r+\gamma}(\mathbf{x}_r)} \tilde{B}_{m-1}(2\gamma). \end{aligned} \quad (4.6)$$

The corresponding steady-state moments are then given by

$$B_m^* = \frac{\tilde{B}_{m-1}(\gamma)}{T_r(\mathbf{x}_r)}. \quad (4.7)$$

A general result that emerges from this analysis is that the statistics of resource accumulation in the presence of exponential resetting is determined completely in terms of the MFPT at two different resetting rates:  $r$  and  $r + \gamma$ , where  $\gamma$  is the degradation rate. In particular, the steady-state mean and variance of the number of packets in the target become

$$\bar{N} = \frac{1}{\gamma T_r(\mathbf{x}_r)}, \quad (4.8)$$

and

$$\text{Var}[N] = \frac{1}{\gamma^2 T_r(\mathbf{x}_r)} \left[ \gamma + \frac{1}{T_{r+\gamma}(\mathbf{x}_r)} - \frac{1}{T_r(\mathbf{x}_r)} \right]. \quad (4.9)$$

(Since the expression for the mean  $\bar{N}$  is an example of Little's law [45], it also holds in the case of nonexponential resetting and delays due to finite return times and refractory periods.) Moreover, the square of the coefficient of variation (CV) satisfies

$$CV^2 = \frac{\text{Var}[N]}{\bar{N}^2} = \frac{T_r(\mathbf{x}_r)}{T_{r+\gamma}(\mathbf{x}_r)} + \gamma T_r(\mathbf{x}_r) - 1, \quad (4.10)$$

and the Fano factor (FF) is given by

$$FF = \frac{\text{Var}[N]}{\bar{N}} = 1 + \frac{1}{\gamma T_{r+\gamma}(\mathbf{x}_r)} - \frac{1}{\gamma T_r(\mathbf{x}_r)}. \quad (4.11)$$

A number of general observations can now be made. Clearly both the mean and variance vanish in the limit  $\gamma \rightarrow \infty$  for fixed  $r$ , since resources delivered to the target are immediately degraded so that there is no accumulation. In addition,  $\lim_{\gamma \rightarrow \infty} T_{r+\gamma}(\mathbf{x}_r) = \infty$ , that is, if the particle resets too frequently, then it never has a chance to reach the target. Equations (4.10) and (4.11) then imply that

$$\lim_{\gamma \rightarrow \infty} CV = \lim_{\gamma \rightarrow \infty} \sqrt{\gamma T_r(\mathbf{x}_r)} = \infty, \quad \lim_{\gamma \rightarrow \infty} FF = 1. \quad (4.12)$$

In the limit of slow degradation,  $\gamma \rightarrow 0$ , we find that the mean and variance both become infinite, which is expected as resources continue to accumulate with little degradation. Indeed, in the absence of degradation there is no steady-state distribution of resources. Also note that

$$\lim_{\gamma \rightarrow 0} CV = 0, \quad \lim_{\gamma \rightarrow 0} FF = 1 + \frac{d}{dr} \left( \frac{1}{T_r} \right). \quad (4.13)$$

Furthermore, Eq. (4.11) implies that if  $\gamma > 0$ , then deviations of FF from unity (Poisson-like noise) simply depends on the difference in  $\bar{N}$  at the resetting rates  $r$  and  $r + \gamma$ . In all of the examples considered in Sec. V, this difference tends to be relatively small so that FF remains in a neighborhood of unity over a wide range of parameters, which means that  $CV \sim 1/\sqrt{\bar{N}}$ . Finally, differentiating both sides of Eq. (4.10) with respect to  $\gamma$  for fixed  $r$  shows that

$$\frac{dCV^2}{d\gamma} = T_r \left[ 1 - \frac{T'_{r+\gamma}}{T_{r+\gamma}^2} \right]. \quad (4.14)$$

The CV will be an increasing function of  $\gamma$  provided that  $T'_{r+\gamma} < T_{r+\gamma}^2$ , which is equivalent to the condition  $\frac{d}{dr} T_{r+\gamma}^{-1} > -1$ .

Now suppose that we vary the resetting rate  $r$  for fixed  $\gamma$  and  $\mathbf{x}_r$ . Equations (4.8) and (4.9) and the condition  $\lim_{r \rightarrow \infty} T_r = \infty$  imply that the mean and variance both vanish in the large- $r$  limit. Again, in the case of fast resetting, the particle rarely has the chance to deliver resources and so degradation dominates. Moreover,

$$\lim_{r \rightarrow \infty} CV = \infty, \quad \lim_{r \rightarrow \infty} FF = 1. \quad (4.15)$$

The behavior when  $r \rightarrow 0$  will depend on whether the MFPT without resetting,  $T_0(\mathbf{x}_r)$ , is finite. If  $\lim_{r \rightarrow 0} T_r(\mathbf{x}_r) = \infty$ , then the mean and variance both vanish, whereas

$$\lim_{r \rightarrow 0} CV = \infty, \quad \lim_{r \rightarrow 0} FF = 1 + \frac{1}{\gamma T_\gamma(\mathbf{x}_r)}. \quad (4.16)$$

On the other hand, if  $T_0(\mathbf{x}_r)$  is finite, then both  $\bar{N}$  and  $\text{Var}[N]$  have finite nonzero values such that

$$\lim_{r \rightarrow 0} CV^2 = \frac{T_0(\mathbf{x}_r)}{T_\gamma(\mathbf{x}_r)} + \gamma T_0(\mathbf{x}_r) - 1, \quad (4.17)$$

and

$$\lim_{r \rightarrow 0} FF = 1 + \frac{1}{\gamma T_\gamma(\mathbf{x}_r)} - \frac{1}{\gamma T_0(\mathbf{x}_r)}. \quad (4.18)$$

It is well known that for a wide range of search processes the MFPT is a unimodal function of the resetting rate  $r$  with a

unique minimum at  $r = r_{\text{opt}}(\mathbf{x}_r)$  [1]:

$$\left. \frac{dT_r(\mathbf{x}_r)}{dr} \right|_{r=r_{\text{opt}}(\mathbf{x}_r)} = 0, \quad \left. \frac{d^2T_r(\mathbf{x}_r)}{dr^2} \right|_{r=r_{\text{opt}}(\mathbf{x}_r)} > 0. \quad (4.19)$$

In the case of diffusion in unbounded domains  $\mathcal{U} \subseteq \mathbb{R}^d$ , this reflects the fact that the MFPT without resetting,  $T_0(\mathbf{x}_0)$ , is infinite for all initial positions  $\mathbf{x}_0 \notin \mathcal{U}_0$ . On the other hand, for diffusion in bounded domains and potential landscapes, one often finds that  $T_r(\mathbf{x}_r)$  can be either a unimodal or a monotonically increasing function of  $r$ , depending on  $\mathbf{x}_r$  [9–11]. Within the context of multiple search-and-capture events with resetting, the steady-state mean number of resources  $\bar{N}$  is inversely proportional to the MFPT  $T_r(\mathbf{x}_r)$ , see Eq. (4.8). This implies that if there exists an optimal resetting rate  $r_{\text{opt}}(\mathbf{x}_r)$  for a given  $\mathbf{x}_r$  then  $\bar{N}$  has a maximum at the same resetting rate.

Given the  $r$ -dependent function  $T_r(\mathbf{x}_r)$  for fixed  $\mathbf{x}_r$ , we would like to derive conditions for the corresponding CV and FF to have at least one stationary point. (In principle, there could be more than one stationary point. However, in the examples explored in Sec. V, there is at most one such point and, if it exists, it corresponds to a minimum.) Differentiating  $CV^2$  with respect to  $r$  for fixed  $\gamma$  and reset position  $\mathbf{x}_r$  yields

$$\frac{dCV^2}{dr} = \gamma \frac{dT_r}{dr} + \frac{1}{T_{r+\gamma}} \frac{dT_r}{dr} - \frac{T_r}{T_{r+\gamma}^2} \frac{dT_{r+\gamma}}{dr}. \quad (4.20)$$

The squared CV will have a stationary point at  $r = r^*$  such that

$$\left. \frac{1}{T_r} \frac{dT_r}{dr} \right|_{r=r^*} = \left. \frac{\Lambda_{r+\gamma}}{T_{r+\gamma}} \frac{dT_{r+\gamma}}{dr} \right|_{r=r^*}, \quad (4.21)$$

where

$$\Lambda_{r+\gamma} = \frac{1}{(\gamma T_{r+\gamma} + 1)} < 1, \quad \gamma > 0. \quad (4.22)$$

Using partial fractions this condition can also be rewritten as

$$\left. \frac{d \ln T_r}{dr} \right|_{r=r^*} = \left[ \frac{d \ln T_{r+\gamma}}{dr} - \frac{d \ln(\gamma T_{r+\gamma} + 1)}{dr} \right] \Big|_{r=r^*}. \quad (4.23)$$

The existence of a stationary point can then be determined by plotting  $\ln T_r$  as a function of  $r$  and using a tangent construction as illustrated in Fig. 4(a) in the case of a unimodal MFPT  $T_r$ . Also note that for large  $\gamma$ , we have  $T'_r \approx 0$  at  $r = r^*$  so that  $r^* \approx r_{\text{opt}}$ . Proceeding in a similar fashion, we can differentiate the Fano factor with respect to  $r$  for fixed  $\gamma$  and reset position  $\mathbf{x}_r$ :

$$\frac{dFF}{dr} = \frac{1}{\gamma} \frac{dT_{r+\gamma}^{-1}}{dr} - \frac{1}{\gamma} \frac{dT_r^{-1}}{dr}. \quad (4.24)$$

The Fano factor will have a stationary point at  $r = r^*$  if

$$\left. \frac{dT_{r+\gamma}^{-1}}{dr} \right|_{r=r^*} = \left. \frac{dT_r^{-1}}{dr} \right|_{r=r^*}. \quad (4.25)$$

The existence of a stationary point can then be determined by plotting  $1/T_r$  as a function of  $r$  and using a tangent construction as illustrated in Fig. 4(b) in the case of a unimodal MFPT  $T_r$ . Note that the curve has to have a mixture of convex and concave sections in order for Eq. (4.25) to be satisfied.

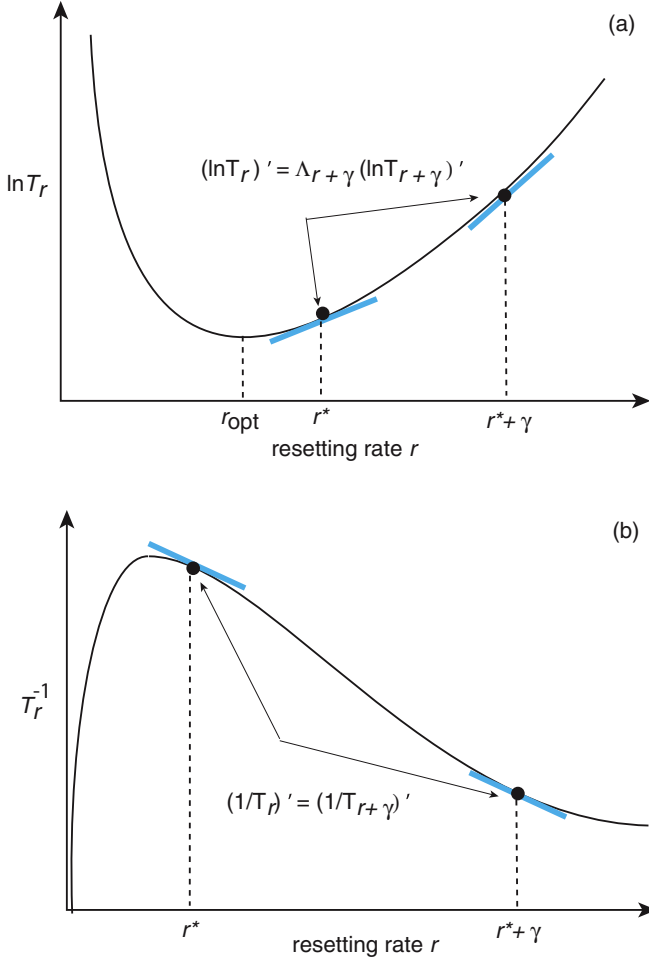


FIG. 4. Tangent constructions for a unimodal MFPT  $T_r$ . (a) Sketch of  $\ln T_r$  as a function of  $r$ . There exists an optimal resetting rate  $r_{\text{opt}}$  such that  $d \ln T_r / dr < 0$  for  $r < r_{\text{opt}}$  and  $d \ln T_r / dr > 0$  for  $r > r_{\text{opt}}$ . The CV has a minimum at  $r = r^*$  such that Eq. (4.21) holds. (b) Sketch of  $T_r^{-1}$  as a function of  $r$ . The FF has a minimum at  $r = r^*$  such that Eq. (4.25) holds.

### B. Effects of refractory delays

It is straightforward to extend the above analysis to incorporate delays arising from refractory resetting and loading or unloading of resources. Setting  $\tilde{\mathcal{F}}(s) = \tilde{f}_r(\mathbf{x}_r, s)\tilde{\rho}(s)$ , Eqs. (3.13) and (3.14) reduce to

$$\begin{aligned} T_r(\mathbf{x}_r) &= \frac{\tilde{Q}_0(\mathbf{x}_r, r) + r\tau_{\text{ref}}\tilde{Q}_0(\mathbf{x}_r, r)}{1 - r\tilde{Q}_0(\mathbf{x}_r, r)} \\ &= \frac{1 + r\tau_{\text{ref}}}{r} \frac{1 - \tilde{f}_0(\mathbf{x}_r, r)}{\tilde{f}_0(\mathbf{x}_r, r)} \\ &= (1 + r\tau_{\text{ref}})\bar{T}_r(\mathbf{x}_r), \end{aligned} \quad (4.26)$$

where  $\bar{T}_r$  denotes the corresponding MFPT without a refractory period, and

$$\begin{aligned} \tilde{f}_r(\mathbf{x}_r, s) &= \frac{1 - (r+s)\tilde{Q}_0(\mathbf{x}_r, r+s)}{1 - r\tilde{\phi}(s)\tilde{Q}_0(\mathbf{x}_r, r+s)} \\ &= \frac{(r+s)\tilde{f}_0(\mathbf{x}_r, r+s)}{r+s - r\tilde{\phi}(s) + r\tilde{\phi}(s)\tilde{f}_0(\mathbf{x}_r, r+s)}. \end{aligned} \quad (4.27)$$

The factor in Eq. (2.21) for  $s = \gamma$  becomes

$$\begin{aligned} &\frac{\tilde{\mathcal{F}}(\gamma)}{1 - \tilde{\mathcal{F}}(\gamma)} \\ &= \frac{\tilde{f}_r(\mathbf{x}_r, \gamma)\tilde{\rho}(\gamma)}{1 - \tilde{f}_r(\mathbf{x}_r, \gamma)\tilde{\rho}(\gamma)} \\ &= \frac{(r+\gamma)\tilde{f}_0(\mathbf{x}_r, r+\gamma)\tilde{\rho}(\gamma)}{\gamma + r[1 - \tilde{\phi}(\gamma)] - [(r+\gamma)\tilde{\rho}(\gamma) - r\tilde{\phi}(\gamma)]\tilde{f}_0(\mathbf{x}_r, r+\gamma)} \\ &= \frac{\tilde{\rho}(\gamma)}{1 - \tilde{\rho}(\gamma) + \{\gamma + r[1 - \tilde{\phi}(\gamma)]\}\bar{T}_{r+\gamma}(\mathbf{x}_r)}. \end{aligned} \quad (4.28)$$

Equations (2.25) and (2.27) then imply that the steady-state mean and variance are given by

$$\bar{N} = \frac{1}{\gamma} \frac{1}{(1 + r\tau_{\text{ref}})\bar{T}_r(\mathbf{x}_r) + \tau_{\text{cap}}}, \quad (4.29)$$

and

$$\begin{aligned} \text{Var}[N] &= \frac{\bar{N}\tilde{\rho}(\gamma)}{1 - \tilde{\rho}(\gamma) + \{\gamma + r[1 - \tilde{\phi}(\gamma)]\}\bar{T}_{r+\gamma}(\mathbf{x}_r)} \\ &\quad + \bar{N}(1 - \bar{N}). \end{aligned} \quad (4.30)$$

It immediately follows from Eq. (4.29) that the introduction of delays decreases the mean  $\bar{N}$ . Moreover, outside the small- $r$  regime, refractory delays following a resetting event without capture will reduce  $\bar{N}$  more strongly than a delay following a single search-and-capture event. The dependence of the CV or FF on refractory delays is more complicated, and will be explored further using a specific example in Sec. V.

## V. EXAMPLES

We now illustrate the theory by considering several different search processes. We use dimensionless units throughout, with the timescale set by the resetting rate  $r$  and the length scale specified by some transport coefficient such as the diffusivity or speed of ballistic transport.

### A. Diffusion on the half-line

For our first example, consider a particle diffusing on the half-line with a target at  $x = 0$ . The survival probability  $\underline{Q}_0$  takes the form of an error function,  $\underline{Q}_0(x_r, t) = \text{erf}(x_r/2\sqrt{Dt})$ , whose Laplace transform is

$$\tilde{Q}_0(x_r, s) = \frac{1 - e^{-\sqrt{s/D}x_r}}{s}. \quad (5.1)$$

Equation (4.1) then implies that [2,3]

$$T_r(x_r) = \frac{1}{r}(e^{\sqrt{r/D}x_r} - 1). \quad (5.2)$$

Note that in the limit  $r \rightarrow 0$ , the MFPT diverges as  $T_r \sim \sqrt{r}$ , which recovers the result that the MFPT of a Brownian particle without resetting to return to the origin is infinite.  $T_r$  also diverges in the limit  $r \rightarrow \infty$  and has a finite and unique minimum at an intermediate value of the resetting rate  $r$  [2,3]. Substituting Eq. (5.2) for  $T_r(x_r)$  into Eqs. (4.8) and (4.9) gives

$$\bar{N} = \frac{r}{\gamma} \frac{1}{e^{\sqrt{r/D}x_r} - 1}, \quad (5.3)$$



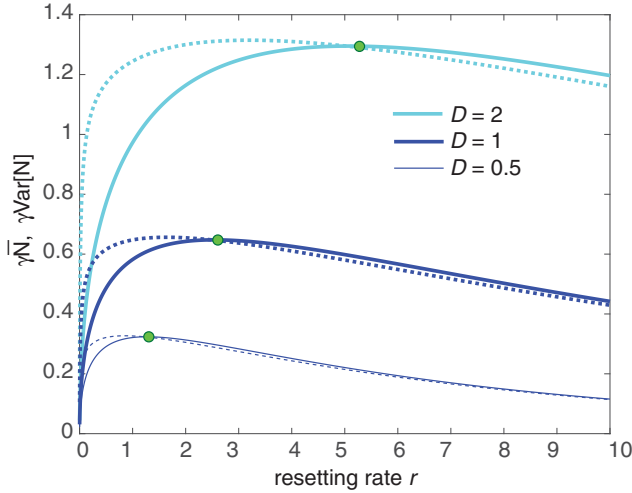


FIG. 5. Particle diffusing on the half-line and searching for a target at the origin. Plot of scaled steady-state mean  $\gamma \bar{N}$  (solid curves) and variance  $\gamma \text{Var}[N]$  (dashed curves) as functions of the resetting rate  $r$  for various diffusivities  $D$ . The reset position is  $x_r = 1$ . Solid (green) dots indicate maxima of the mean curves at  $r = r_{\text{opt}}$ . For the variance we take  $\gamma = 0.1$ .

and

$$\text{Var}[N] = \frac{r}{\gamma^2} \frac{1}{e^{\sqrt{r/D}x_r} - 1} \times \left[ \frac{\gamma e^{\sqrt{(r+\gamma)/D}x_r} + r}{e^{\sqrt{(r+\gamma)/D}x_r} - 1} - \frac{r}{e^{\sqrt{r/D}x_r} - 1} \right]. \quad (5.4)$$

In Fig. 5 we show plots of the mean  $\bar{N}$  (scaled by a factor  $\gamma$ ) as a function of the resetting rate  $r$  for various diffusivities. (Under the rescaling, the plots are independent of the degradation rate  $\gamma$ .) As expected, the maximum of the mean number of packets occurs at the optimal resetting rate  $r_{\text{opt}}$  for minimizing  $T_r$  (for given  $D$  and  $x_r$ ). The maximum is an increasing function of  $D$  since a faster search process means that the target receives resources at a faster mean rate. In Fig. 6 we show corresponding plots of the FF against  $r$  for various  $D$  and  $\gamma$ . Consistent with Eqs. (4.16) and (4.17), the Fano factor has a finite value at  $r = 0$  and asymptotes to  $FF = 1$  as  $r \rightarrow \infty$ . Moreover, each of the curves has a unique minimum satisfying the condition (4.25). As  $\gamma \rightarrow \infty$ , the FF curves approach the straight line  $FF = 1$  as indicated by Eq. (4.13). Indeed, for  $\gamma > 0$  and sufficiently fast resetting the FF curves tend to lie in a neighborhood of unity, indicating Poisson-like noise. When  $\gamma \rightarrow 0$ , the FF curve diverges at  $r = 0$  since  $dT_r^{-1}/dr \rightarrow \infty$ , see condition (4.13). Finally, plots of the CV for  $\gamma = 1$  and  $\gamma = 0.1$  are displayed in Fig. 7. Again consistent with Eqs. (4.16) and (4.17), the CV has the limits  $CV \rightarrow \infty$  for  $r \rightarrow 0$  and  $r \rightarrow \infty$ . Each CV curve has a minimum at a  $\gamma$ -dependent resetting rate  $r^*(\gamma)$  where the condition (4.21) holds; the dependence of the minimum on  $\gamma$  is indicated by the arrows in Fig. 6. It can also be seen that increasing  $\gamma$  shifts the CV curves upward, which reflects the fact that  $FF \approx 1$  and  $\bar{N}$  decreases with increasing  $\gamma$ .

We can also use the example of diffusion on the half-line to illustrate the effects of refractory periods on the accumulation of resources at the target. For concreteness, suppose that  $\rho$  and

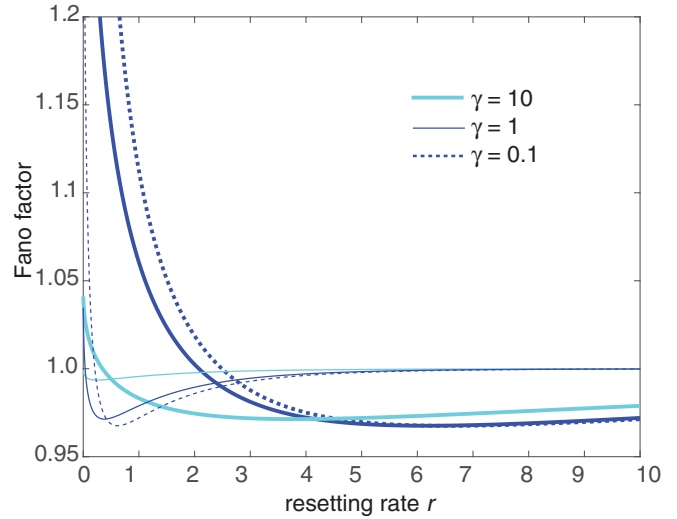


FIG. 6. Particle diffusing on the half-line and searching for a target at the origin. Plot of the Fano factor (FF) as a function of the resetting rate  $r$  for various  $\gamma$ . The reset position is  $x_r = 1$  and the diffusivity is  $D = 1$  (thick curves) or  $D = 0.1$  (thin curves).

$\phi$  are exponential waiting time densities so

$$\tilde{\rho}(s) = \frac{1}{1 + s\tau_{\text{cap}}}, \quad \tilde{\phi}(s) = \frac{1}{1 + s\tau_{\text{ref}}}. \quad (5.5)$$

Example plots of the scaled mean, the FF and CV are shown in Figs. 8–10, respectively. As expected, the introduction of delays reduces the mean, and the effect is stronger in the case of  $\tau_{\text{ref}}$  for sufficiently large  $r$ . On the other hand, the FF tends to be reduced by delays after capture and to be increased by delays after resetting. We find similar results for different

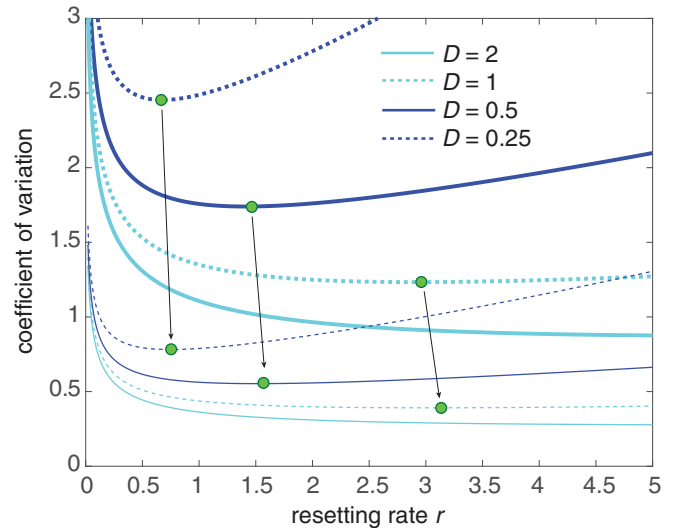


FIG. 7. Particle diffusing on the half-line and searching for a target at the origin. Plot of the coefficient of variation (CV) as a function of the resetting rate  $r$  for various diffusivities  $D$ . The reset position is  $x_r = 1$  and the degradation rate is  $\gamma = 1$  (thick curves) or  $\gamma = 0.1$  (thin curves). Solid (green) dots indicate minima of the CV curves at  $r = r^*(\gamma)$  and the arrows indicate their displacement under the reduction of  $\gamma$ .

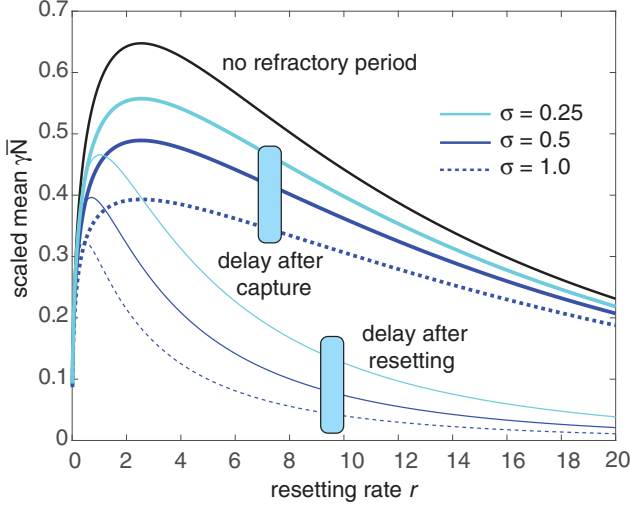


FIG. 8. Particle diffusing on the half-line and searching for a target at the origin. Plot of steady-state mean  $\bar{N}$  (scaled by  $\gamma$ ) as a function of the resetting rate  $r$  for various refractory periods  $\bar{\sigma}$ . Thick curves represent  $\tau_{\text{cap}} = 0$ ,  $\tau_{\text{ref}} = \bar{\sigma}$ , while thin curves represent the case  $\tau_{\text{cap}} = \bar{\sigma}$ ,  $\tau_{\text{ref}} = 0$ . The reset position is  $x_r = 1$  and the diffusivity is  $D = 1$ .

values of  $\gamma$ . Since changes in FF are relatively insensitive to delays, it follows that the effects on the CV are dominated by the corresponding changes in  $\bar{N}$ . Hence, the CV increases in the presence of refractory delays, and again the effect is more pronounced in the case of resetting delays when  $r$  is large.

### B. Velocity jump process

Although we formulated the theory in terms of a scalar master equation (2.1), it is straightforward to extend the analysis to a multivariate master equation. We illustrate this by considering a symmetric velocity jump process [6], which could describe the unbiased growth and shrinkage of microtubules [46] or cytonemes [40], the motion of molecular motors [37], or bacterial run-and-tumble [47]. Let  $p_{\pm}(x, t)$ ,

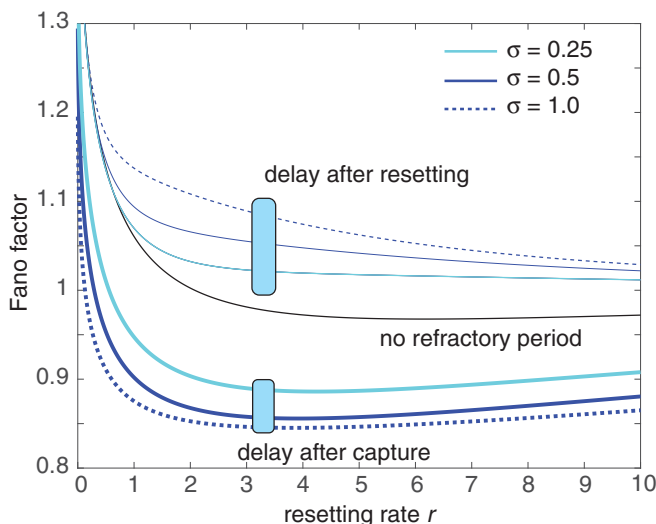


FIG. 9. Corresponding plots of FF for  $\gamma = 1$ .

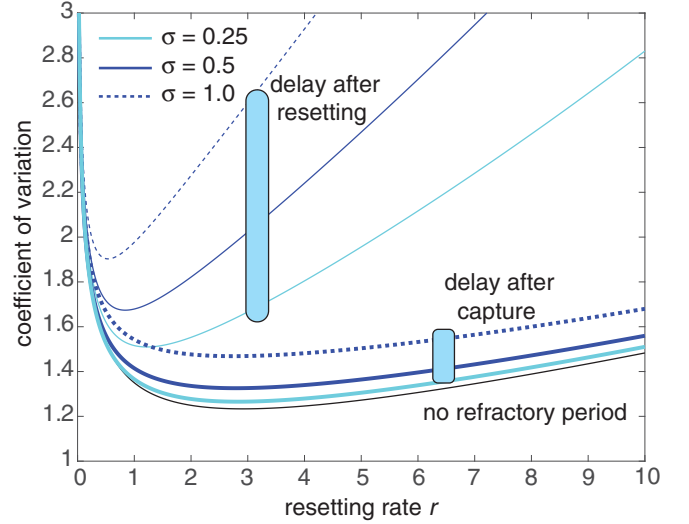


FIG. 10. Corresponding plots of CV for  $\gamma = 1$ .

$x \in \mathbb{R}^+$ , be the probability density of a particle that is moving at constant speed  $\pm v$  and suppose that it reverses direction at a rate  $\alpha$ . In the absence of resetting the master equation takes the form

$$\frac{\partial p_+(x, t)}{\partial t} = -v \frac{\partial p_+(x, t)}{\partial x} - \alpha p_+(x, t) + \alpha p_-(x, t), \quad (5.6a)$$

$$\frac{\partial p_-(x, t)}{\partial t} = v \frac{\partial p_-(x, t)}{\partial x} - \alpha p_-(x, t) + \alpha p_+(x, t), \quad (5.6b)$$

supplemented by an absorbing boundary condition at  $x = 0$ ,  $p_+(0, t) = 0$ . This is a symmetric process, since the antero-grade and retrograde speeds are the same, as are the rates of switching between the two velocity states. It is well known that such a system is equivalent to the telegrapher's equation [48]. Now suppose that stochastic resetting is included along the following lines: With rate  $r$  the particle resets to its initial position  $x_r$  and the velocity is chosen to be  $\pm v$  with equal probability 1/2. Since the resetting protocol preserves the initial conditions, the renewal theory of Sec. III still holds [6]. Hence, as in the previous examples, we need to calculate the Laplace transform of the survival probability without resetting.

Let  $Q_0^{\pm}(x_0, t)$  denote the survival probability without resetting for a particle having started at  $x = x_0$  with initial velocity  $\pm v$ . The total survival probability is then

$$Q_0(x_0, t) = \frac{1}{2}[Q_0^+(x_0, t) + Q_0^-(x_0, t)]. \quad (5.7)$$

The survival probabilities  $Q_0^{\pm}$  satisfy the backward master equation

$$\frac{\partial Q_0^+(x_0, t)}{\partial t} = v \frac{\partial Q_0^+(x_0, t)}{\partial x_0} - \alpha Q_0^+(x_0, t) + \alpha Q_0^-(x_0, t), \quad (5.8a)$$

$$\frac{\partial Q_0^-(x_0, t)}{\partial t} = -v \frac{\partial Q_0^-(x_0, t)}{\partial x_0} - \alpha Q_0^-(x_0, t) + \alpha Q_0^+(x_0, t), \quad (5.8b)$$

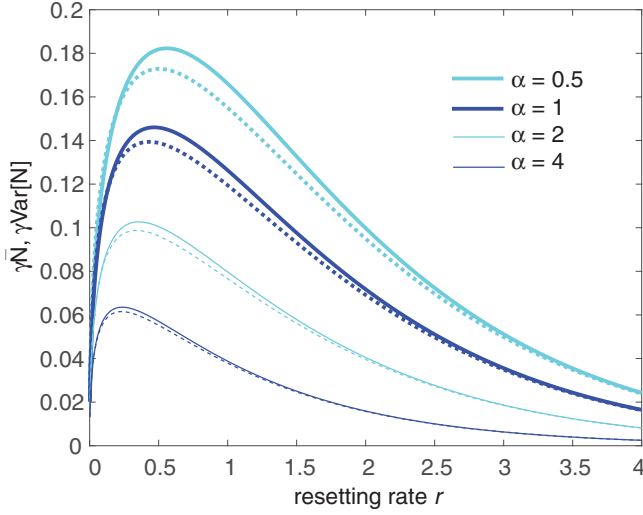


FIG. 11. Velocity jump process on the half-line with a target at  $x = 0$ . Plot of scaled steady-state mean  $\gamma\bar{N}$  (solid curves) and  $\gamma\text{Var}[N]$  (dashed curves) as functions of the resetting rate  $r$  for various switching rates  $\alpha$ . The reset position is  $x_r = 1$  and the speed is  $v = 1$ . For the variance  $\gamma = 0.1$ .

for  $x_0 > 0$  The initial conditions are  $Q_0^\pm(x_0, 0) = 1$ , and there is an absorbing boundary condition at  $x = 0$ ,  $Q_0^-(0, t) = 0$ . Using Laplace transforms, the solution is [6]

$$\tilde{Q}_0(x_0, s) = \frac{1}{s} + \frac{1}{2\alpha s} [v\lambda(s) - (s + 2\alpha)]e^{-\lambda(s)x_0}, \quad (5.9)$$

where

$$\lambda(s) = \sqrt{\frac{s(s + 2\alpha)}{v^2}}. \quad (5.10)$$

This can then be substituted into Eq. (4.1), and used to calculate the mean and variance according to Eqs. (4.8) and (4.9). In Figs. 11 and 12 we show plots of the scaled mean  $\gamma\bar{N}$ , the scaled variance  $\gamma\text{Var}[N]$  and the CV as functions of the resetting rate  $r$  for various switching rates  $\alpha$  and  $x_r = 1 = v$ . (As in the previous example  $FF \sim 1$ .) We observe the same qualitative behavior as in the previous two examples. Note that reducing the switching rate  $\alpha$  increases the mean and reduces the CV. Again the results are consistent with the general analysis of Sec. IV, with  $\alpha$  analogous to the diffusivity.

### C. Diffusion on an interval

In the above two examples the MFPT without resetting is infinite for all reset positions  $x_r > 0$ ,  $T_0(x_r) = \infty$ . We now consider an example where  $T_0(x_r)$  is finite and  $T_r(x_r)$  may either be a unimodal function of  $r$  or a monotonically increasing function of  $r$ , depending on the reset location  $x_r$ . Various examples of this situation have been considered elsewhere [9, 11–13]. Here we will focus on the simple case of Brownian motion in the finite interval  $[0, L]$  with a target at  $x = 0$  and a reflecting boundary at  $x = L$ . In the absence of resetting the Laplace transformed survival probability  $\tilde{Q}_0(x, s)$  satisfies the equation

$$D \frac{d^2 \tilde{Q}_0}{dx^2} - s \tilde{Q}_0 = -1, \quad x \in (0, L), \quad (5.11)$$

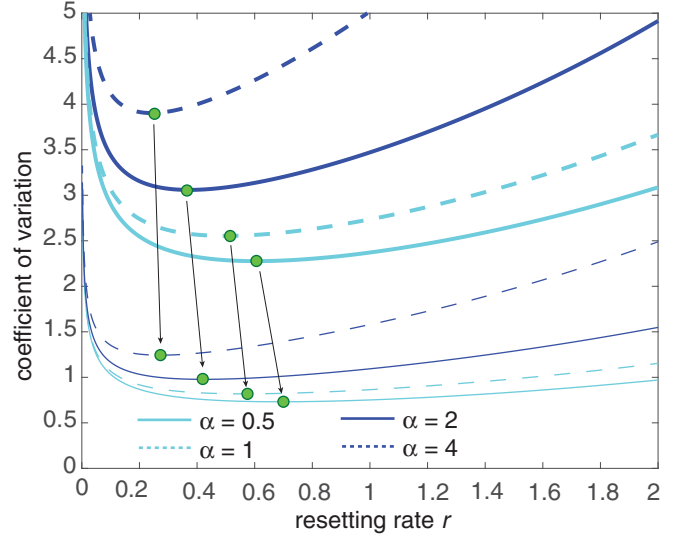


FIG. 12. Velocity jump process on the half-line with a target at  $x = 0$ . Plot of coefficient of variation as a function of the resetting rate  $r$  for various switching rates  $\alpha$ . The reset position is  $x_r = 1$ , the speed is  $v = 1$  and the degradation rate is  $\gamma = 1$  (thick curves) or  $\gamma = 0.1$  (thin curves). Solid (green) dots indicate minima of CV curves and the arrows indicate their displacement under the reduction of  $\gamma$ .

together with the boundary conditions

$$\tilde{Q}_0(0, s) = 0, \quad \partial_x \tilde{Q}_0(L, s) = 0. \quad (5.12)$$

The solution takes the form

$$\tilde{Q}_0(x, s) = \frac{1}{s} \left\{ 1 - \frac{\cosh(\sqrt{s/D}[L - x])}{\cosh(\sqrt{s/D}L)} \right\}. \quad (5.13)$$

Taking the limit  $s \rightarrow 0$  and using L'Hopital's rule yields the classical results

$$T_0(x) = -\frac{x^2}{2D} + \frac{xL}{D},$$

$$T_0^{(2)}(x) = \frac{1}{12D^2}(x^4 - 4x^3L + 8xL^3). \quad (5.14)$$

Here  $T_0^{(2)}$  is the second moment of the FPT density without resetting. Equation (4.1) then implies that [10]

$$T_r(x_r) = \frac{\cosh(\sqrt{r/D}L) - \cosh(\sqrt{r/D}[L - x_r])}{r \cosh(\sqrt{r/D}[L - x_r])}. \quad (5.15)$$

Note that in the limit  $r \rightarrow 0$ ,  $T_r(x_r) \rightarrow T_0(x_r)$ , whereas  $T_r(x_r) \rightarrow \infty$  as  $r \rightarrow \infty$ .

One finds that the MFPT  $T_r(x_r)$  is a unimodal function of  $r$  for reset locations close to the target and a monotonically increasing function of  $r$  at more distal locations, as illustrated in Fig. 13; in the former case there exists an optimal resetting rate that minimizes  $T_r$ . One way to investigate whether or not the MFPT has at least one turning point is to calculate the sign of the derivative  $dT_r/dr$  at  $r = 0$  [24–26, 28]. If this derivative is negative, then resetting reduces the MFPT in the

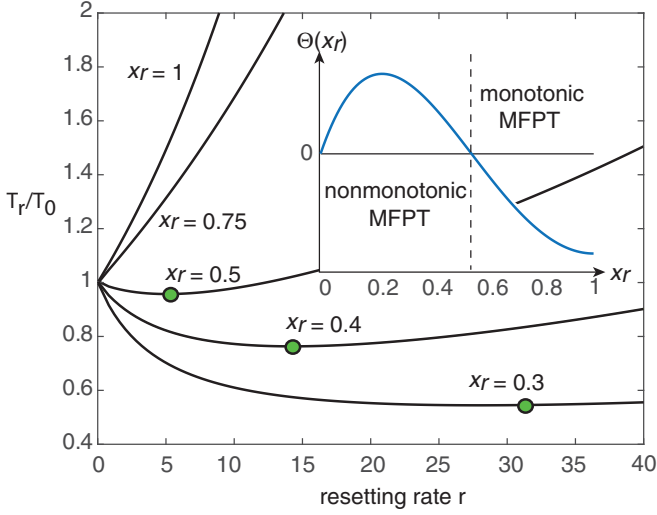


FIG. 13. Plot of  $T_r(x_r)/T_0(x_r)$  as a function of the resetting rate  $r$  for various reset positions  $x_r$ . Other parameters are  $L = 1 = D$ . The solid (green) dots indicate the optimal resetting rate for a given  $x_r$ . Inset: Plot of  $\Theta(x_r) := \tau^{(2)}(x_r) - 2\tau(x_r)^2$  as a function of the reset location  $x_r$ . Here  $\tau$  and  $\tau^{(2)}$  are the MFPT and second moment in the absence of resetting. The sign of  $\Theta$  determines whether or not the corresponding MFPT with resetting is initially a decreasing function of the resetting rate  $r$ .

small- $r$  regime. Equation (4.1) implies that

$$\begin{aligned} T_r'(\mathbf{x}_r) &= \tilde{Q}_0'(\mathbf{x}_r, 0) + \tilde{Q}_0(\mathbf{x}_r, 0)^2 \\ &= T_0(\mathbf{x}_r)^2 - \frac{T_0^{(2)}(\mathbf{x}_r)}{2}. \end{aligned} \quad (5.16)$$

Introducing the variance  $\sigma_0^2(\mathbf{x}_r) = T_0^{(2)}(\mathbf{x}_r) - T_0(\mathbf{x}_r)^2$ , it follows that adding a small rate of resetting reduces the MFPT for a given  $\mathbf{x}_r$  if and only if

$$\frac{\sigma_0(\mathbf{x}_r)}{T_0(\mathbf{x}_r)} > 1. \quad (5.17)$$

In the inset of Fig. 13 we plot  $\Theta(x_r) := T_0^{(2)}(x_r) - 2T_0(x_r)^2$  as a function of  $x_r$ , with  $T_0(x_r)$ ,  $T_0^{(2)}(x_r)$  defined in Eq. (5.14). Applying the condition (5.17) implies that the sign of  $\Theta$  determines whether the corresponding MFPT  $T_r$  with resetting is initially a decreasing function of the resetting rate  $r$ . It can be seen that  $\Theta(x_r)$  is negative in the case of proximal positions ( $x_r < x_c \approx 0.55$ ) but switches to positive values in the case of distal locations ( $x_r > x_c$ ). In Fig. 14 we show example plots of the CV as a function of the resetting rate and various restart positions  $x_r$ . We find that the CV is a unimodal function of  $r$  for  $x_r < x_c$  and a monotonically increasing function of  $r$  for  $x_r > x_c$ . The latter is a consequence of the fact that in this regime the curve  $1/T_r$  is everywhere concave, see Eq. (4.25). Moreover, consistent with Eq. (4.17), the CV has a finite limit as  $r \rightarrow 0$ , which for the given parameters is only weakly dependent on  $x_r$ . The FF also switches from unimodal to monotonic behavior as  $x_r$  increases but the transition point is above  $x_c$ , as can be seen in Fig. 15 for  $x = 0.6 > x_c$ . It can be checked that although  $1/T_r$  is a monotonically decreasing function of  $r$  at  $x_r = 0.6$ , it switches from a concave to a convex function, consistent with Eq. (4.25).

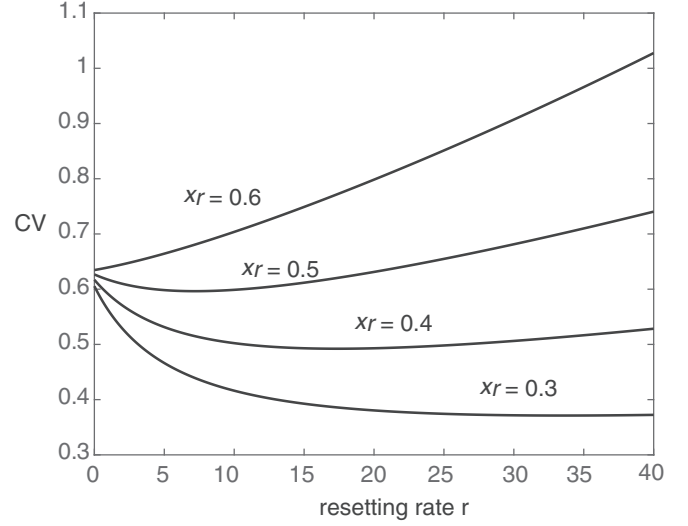


FIG. 14. Particle diffusing on the finite interval  $[0, L]$  with an absorbing target at the origin and a reflecting boundary at  $x = L$ . Plot of CV as a function of the resetting rate  $r$  for various reset points  $x_r$ . Other parameters are  $D = L = 1 = \gamma$ .

#### D. Diffusive search for a spherical target

As our final example, we consider a Brownian particle searching for a  $d$ -dimensional, spherical target in an unbounded domain. The FPT for a single search-and-capture event with resetting was analyzed in Ref. [4]. In particular, one can exploit spherical symmetry by taking the center of the target to be at the origin so that the solution for the survival probability and moments of the FPT density only depend on the radial distance  $x = |\mathbf{x}|$  of the initial position or reset point and the radius  $a$  of the sphere. The Laplace transformed

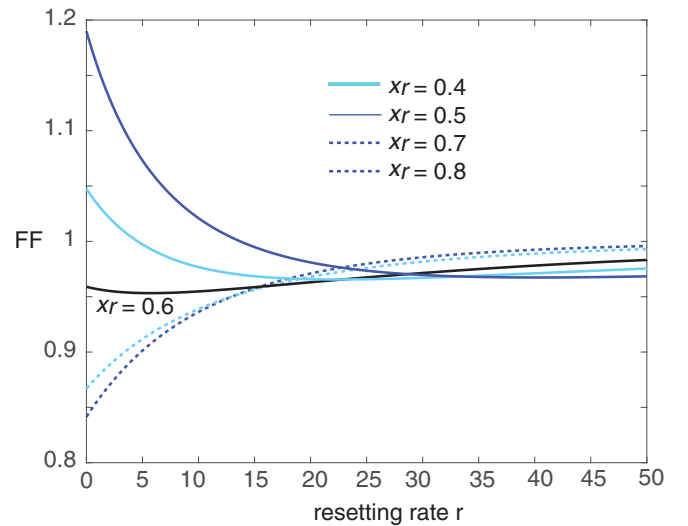


FIG. 15. Particle diffusing on the finite interval  $[0, L]$  with an absorbing target at the origin and a reflecting boundary at  $x = L$ . Plot of FF as a function of the resetting rate  $r$  for various reset points  $x_r$ . Other parameters are  $D = L = 1 = \gamma$ .

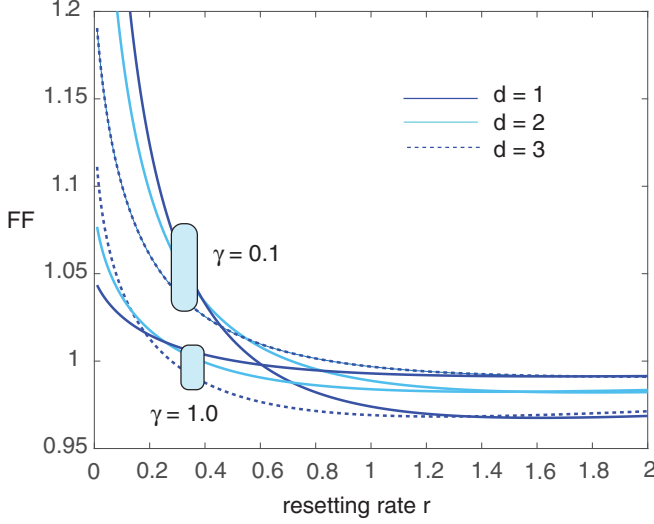


FIG. 16. Diffusive search for a spherical target of radius  $a$  in  $\mathbb{R}^d$ . Plot of FF as a function of the resetting rate  $r$  for  $x_r = 3$  and  $d = 1, 2, 3$ . The lower and upper three curves correspond to  $\gamma = 0.1$  and  $\gamma = 1.0$ , respectively. Other parameters are  $a = 1 = D$ .

survival probability without resetting evolves according to

$$\frac{d^2 \tilde{Q}_0}{dx^2} + \frac{d-1}{x} \frac{d\tilde{Q}_0}{dx} - s\tilde{Q}_0 = -1, \quad a < x < \infty, \quad (5.18)$$

together with the boundary condition  $\tilde{Q}_0(a, s) = 0$ . Following Ref. [4], the solution takes the form

$$\tilde{Q}_0(x, s) = \frac{1}{s} \left[ 1 - \frac{x^\nu K_\nu(\sqrt{s/D}x)}{a^\nu K_\nu(\sqrt{s/D}a)} \right], \quad (5.19)$$

where  $\nu = 1 - d/2$  and  $K_\nu$  is the modified Bessel function of the second kind of order  $\nu$ . Substituting Eq. (5.19) into (4.1) leads to the following expression for the MFPT  $T_r$  [4]:

$$T_r(x_r) = \frac{a^\nu K_\nu(\sqrt{r/D}a) - x_r^\nu K_\nu(\sqrt{r/D}x_r)}{rx_r^\nu K_\nu(\sqrt{r/D}x_r)}. \quad (5.20)$$

The qualitative behavior of the mean  $\bar{N}$  and variance is the same as the first example of diffusion on the half-line. Therefore, here we focus on how the FF and CV and FF depend on the dimension  $d$  for different values of  $\gamma$ . Example plots of the FF are shown in Fig. 16 for  $\gamma = 0.1$ . Again  $FF \approx 1$  except when  $r$  or  $\gamma$  is sufficiently small. On the other hand, the CV appears to be much more sensitive to both the dimension and the degradation rate as illustrated in Fig. 17. This reflects a corresponding parameter dependence for  $\bar{N}$ .

## VI. MULTIPLE PACKETS AND NOISE REDUCTION

All of the examples considered in Sec. V exhibited significant fluctuations. One way to reduce fluctuations is to assume that during each burst event, the particle delivers  $d$  packets that degrade independently. In order to establish this result, it is necessary to modify the analysis of the binomial moments in Sec. II. The number of packets at the target at time  $t$  is now

$$N(t) = \sum_{n, 0 \leq T_n \leq t} \sum_{i=1}^d I(t - T_n, S_{ni}), \quad (6.1)$$

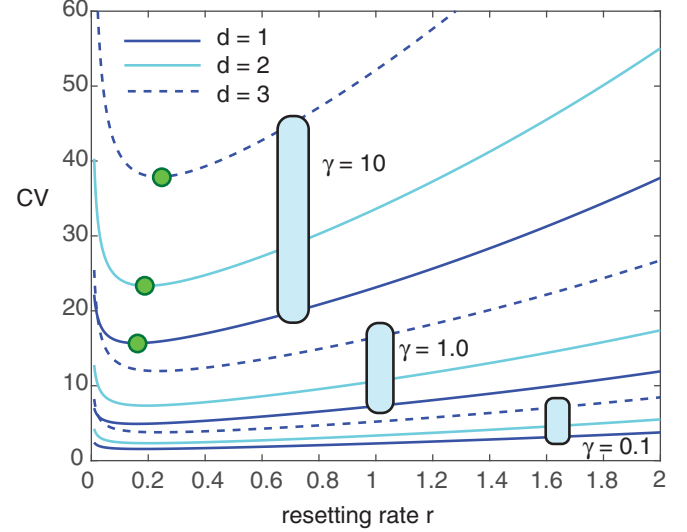


FIG. 17. Diffusive search for a spherical target of radius  $a$  in  $\mathbb{R}^d$ . Plot of CV as a function of the resetting rate  $r$  for  $x_r = 5$  and  $d = 1, 2, 3$ . The lower, middle and upper three curves correspond to  $\gamma = 0.1$ ,  $\gamma = 1.0$  and  $\gamma = 10.0$ , respectively. Other parameters are  $a = 1 = D$ .

where  $S_{ni}$ ,  $i = 1, \dots$ , is the service time of the  $i$ th member of the  $n$ th burst event. Since  $I(t - y, S_{li})$  for  $i = 1, 2, \dots, d$  are independent and identically distributed, the total expectation theorem yields

$$\begin{aligned} \mathbb{E}[z^{\sum_{i=1}^d I(t - T_n, S_{ni})}] &= \mathbb{E} \left[ \prod_{i=1}^d \mathbb{E}[z^{I(t - y, S_{li})}] \right] \\ &= \int_0^\infty [z + (1 - z)\Phi(t - y)]^d dF(y). \end{aligned} \quad (6.2)$$

We have used Eq. (2.15). Another application of the total expectation theorem gives

$$\begin{aligned} G(z, t) &= \mathbb{E}[z^{N(t)}] = \mathbb{E}[\mathbb{E}[z^{N(t)} | T_1 = y]] \\ &= \int_t^\infty dF(y) \\ &\quad + \int_0^t [z + (1 - z)\Phi(t - y)]^d G(z, t - y) dF(y). \end{aligned} \quad (6.3)$$

Differentiating Eq. (6.3) using

$$\begin{aligned} \frac{d^m}{dz^m} [z + (1 - z)\Phi(t - y)]^d \Big|_{z=1} \\ = \begin{cases} \frac{d!}{(d - m)!} [1 - \Phi(t - y)]^m & \text{if } d \geq m \\ 0 & \text{if } d < m \end{cases}, \end{aligned} \quad (6.4)$$

leads to the following integral equation for the binomial moments:

$$\begin{aligned} B_m(t) &= \int_0^t B_m(t - y) dF(y) + \sum_{l=1}^{\min\{m, d\}} \binom{d}{l} \\ &\quad \times \int_0^t B_{m-l}(t - y) [1 - \Phi(t - y)]^l dF(y). \end{aligned} \quad (6.5)$$

Since  $1 - \Phi(t - y) = e^{-\gamma(t-y)}$ , this can be written in the more compact form

$$B_m(t) = \int_0^t B_m(t-y)dF(y) + \int_0^t \mathcal{H}_m(t-y)dF(y), \quad (6.6)$$

where

$$\mathcal{H}_m(t) = \sum_{l=1}^{\min\{m,d\}} \binom{d}{l} B_{m-l}(t) e^{-l\gamma t}. \quad (6.7)$$

In order to obtain the steady-state binomial moments, we Laplace transform Eq. (6.6) with  $dF(y) = \mathcal{F}(y)dy$ :

$$\tilde{B}_m(s) = \tilde{B}_m(s)\tilde{\mathcal{F}}(s) + \tilde{\mathcal{H}}_m(s)\tilde{\mathcal{F}}(s), \quad (6.8)$$

which can be rearranged to give

$$\begin{aligned} \tilde{B}_m(s) &= \frac{\tilde{\mathcal{H}}_m(s)\tilde{\mathcal{F}}(s)}{1 - \tilde{\mathcal{F}}(s)} \\ &= \frac{\tilde{\mathcal{F}}(s)}{1 - \tilde{\mathcal{F}}(s)} \sum_{l=1}^{\min\{m,d\}} \binom{d}{l} \tilde{B}_{m-l}(s + l\gamma). \end{aligned} \quad (6.9)$$

Multiplying both sides by  $s$  and taking the limit  $s \rightarrow 0^+$  along identical lines to the derivation of Eq. (2.21) yields

$$\begin{aligned} B_m^* &= \lim_{s \rightarrow 0^+} \frac{s\tilde{\mathcal{F}}(s)}{1 - \tilde{\mathcal{F}}(s)} \sum_{l=1}^{\min\{m,d\}} \binom{d}{l} \tilde{B}_{m-l}(l\gamma) \\ &= \frac{\lambda}{\gamma} \sum_{l=1}^{\min\{m,d\}} \binom{d}{l} \tilde{B}_{m-l}(l\gamma). \end{aligned} \quad (6.10)$$

In particular, the mean is

$$B_1^* \equiv \bar{N} = \frac{d\lambda}{\gamma}, \quad (6.11)$$

with  $\lambda$  given by Eq. (2.23). As expected,  $\bar{N}$  scales with the number of packets  $d$  per delivery. Similarly, defining  $H_{m,d} = 1$  if  $m \leq d$  and zero otherwise,

$$\begin{aligned} B_2^* &= \lambda \left[ \tilde{B}_1(\gamma)d + \frac{H_{2,d}d(d-1)}{4\gamma} \right] \\ &= \frac{d^2\lambda}{4\gamma} \left[ \frac{2\tilde{\mathcal{F}}(\gamma)}{1 - \tilde{\mathcal{F}}(\gamma)} + H_{2,d} \right] - \frac{d\lambda H_{2,d}}{4\gamma}. \end{aligned} \quad (6.12)$$

Hence, the variance is

$$\text{var}[N] = C_1 d + C_2 d^2, \quad (6.13)$$

where

$$C_1 = \frac{\lambda}{\gamma} \left( 1 - \frac{H_{2,d}}{2} \right), \quad (6.14)$$

$$C_2 = \frac{\lambda}{2\gamma} \left[ \frac{2\tilde{\mathcal{F}}(\gamma)}{1 - \tilde{\mathcal{F}}(\gamma)} + H_{2,d} \right] - \frac{\lambda^2}{\gamma^2}. \quad (6.15)$$

For  $d \geq 2$  the coefficients are independent of  $d$  so that the  $d$  dependence of the corresponding coefficient of variation (CV) can be expressed as

$$\text{CV} = \frac{\gamma}{\lambda} \sqrt{C_2 + \frac{C_1}{d}}. \quad (6.16)$$

This establishes that increasing  $d$  reduces the CV.

A more effective way to reduce fluctuations is to have  $M$  independent, parallel searchers. Statistical independence implies that the steady-state mean and variance become

$$\bar{N} = \frac{Md\lambda}{\gamma}, \quad (6.17)$$

and

$$\text{Var}[N] = Md(C_2 d + C_1). \quad (6.18)$$

The CV thus scales as

$$\text{CV} = \frac{\gamma}{\lambda\sqrt{Md}} \sqrt{C_2 d + C_1}. \quad (6.19)$$

Note that the steady-state mean  $\bar{N}$  depends on the product  $Md$ . Hence, for a given mean, one can reduce the CV by decreasing  $d$  and increasing  $M$  such that  $Md$  is fixed. That is, a larger number of searchers carrying a smaller number of packets results in smaller fluctuations. (An analogous observation was made in a study of cytoneme-based transport [40].) Finally, note that these scaling arguments still hold if each search-and-capture event involves stochastic resetting.

## VII. DISCUSSION

Motivated by examples of search processes in cell biology, we have developed a general theoretical framework for studying the accumulation of resources in a target due to the sequential delivery of resources via multiple search-and-capture events with resetting, combined with natural degradation. We showed how this problem can be mapped onto a  $G/M/\infty$  queue and used this to derive an integral equation for the binomial moments of the number  $N(t)$  of packets at time  $t$ . Laplace transforming the integral equation allowed us to derive explicit expressions for the mean and variance of  $N(t)$  in steady state, which depend on the resetting rate  $r$  and the degradation rate  $\gamma$ . One of our main findings is that in the case of exponential resetting the mean and variance depend on the MFPTs  $T_r(\mathbf{x}_r)$  and  $T_{r+\gamma}(\mathbf{x}_r)$ . We used this observation to derive general conditions for the CV and FF to have at least one stationary point as functions of  $r$  and to investigate their behavior in the asymptotic limits  $r \rightarrow 0, \infty$  and  $\gamma \rightarrow 0, \infty$ . This was illustrated by considering several specific search processes with exponential resetting. In each case we found that over a large parameter range the noise was Poisson-like with  $FF \approx 1$ .

There are a variety of possible future directions. First, extending the analysis to a wider range of examples that includes finite return times, nonexponential resetting and non-Markovian search processes. A second major extension is to consider resource allocation to multiple competing targets. This type of problem has previously been considered within the specific context of cytoneme-based morphogen transport [19,40], where queuing theory was used to analyze the accumulation of morphogen in a 1D array of target cells. (One major difference from the current paper is that the targets were only partially absorbing.) More recently we have used renewal theory to analyze a single search-and-capture process with noninstantaneous resetting and multiple targets [29], which

could be extended to analyze resource accumulation in a population of targets. The effect of stochastic resetting on search processes with two or more targets has also been considered by a number of other authors [10,25–27,49].

ACKNOWLEDGMENTS

P.C.B. was supported by the National Science Foundation (DMS-1613048). We thank the reviewers for their constructive comments.

---

[1] M. R. Evans, S. N. Majumdar, and G. Schehr, Stochastic resetting and applications, *J. Phys. A* **53**, 193001 (2020).

[2] M. R. Evans and S. N. Majumdar, Diffusion with Stochastic Resetting, *Phys. Rev. Lett.* **106**, 160601 (2011).

[3] M. R. Evans and S. N. Majumdar, Diffusion with optimal resetting, *J. Phys. A: Math. Theor.* **44**, 435001 (2011).

[4] M. R. Evans and S. N. Majumdar, Diffusion with resetting in arbitrary spatial dimension, *J. Phys. A* **47**, 285001 (2014).

[5] L. Kusmierz, S. N. Majumdar, S. Sabhapandit, and G. Schehr, First Order Transition for the Optimal Search Time of Levy Flights with Resetting, *Phys. Rev. Lett.* **113**, 220602 (2014).

[6] M. R. Evans and S. N. Majumdar, Run and tumble particle under resetting: A renewal approach, *J. Phys. A: Math. Theor.* **51**, 475003 (2018).

[7] P. C. Bressloff, Directed intermittent search with stochastic resetting, *J. Phys. A* **53**, 105001 (2020).

[8] P. C. Bressloff, Switching diffusions and stochastic resetting, *J. Phys. A* **53**, 275003 (2020).

[9] S. Ray, M. Mondal, and S. Reuveni, Peclet number governs transition to acceleratory restart in drift-diffusion, *J. Phys. A* **52**, 255002 (2019).

[10] A. Pal, Diffusion in a potential landscape with stochastic resetting, *Phys. Rev. E* **91**, 012113 (2015).

[11] S. Ray and S. Reuveni, Diffusion with resetting in a logarithmic potential, *J. Chem. Phys.* **152**, 234110 (2020).

[12] A. Pal and V. V. Prasad, First passage under stochastic resetting in an interval, *Phys. Rev. E* **99**, 032123 (2019).

[13] X. Durang, S. Lee, L. Lizana, and J.-H. Jeon, First-passage statistics under stochastic resetting in bounded domains, *J. Phys. A: Math. Theor.* **52**, 224001 (2019).

[14] M. R. Evans and S. N. Majumdar, Effects of refractory period on stochastic resetting, *J. Phys. A: Math. Theor.* **52**, 01LT01 (2019).

[15] A. Maso-Puigdellosas, D. Campos, and V. Mendez, Stochastic movement subject to a reset-and-residence mechanism: Transport properties and first arrival statistics, *J. Stat. Mech.* (2019) 033201.

[16] A. Pal, L. Kusmierz, and S. Reuveni, Invariants of motion with stochastic resetting and space-time coupled returns, *New J. Phys.* **21**, 113024 (2019).

[17] A. Maso-Puigdellosas, D. Campos, and V. Mendez, Transport properties of random walks under stochastic noninstantaneous resetting, *Phys. Rev. E* **100**, 042104 (2019).

[18] A. S. Bodrova and I. M. Sokolov, Resetting processes with noninstantaneous return, *Phys. Rev. E* **101**, 052130 (2020).

[19] P. C. Bressloff, Modeling active cellular transport as a directed search process with stochastic resetting and delays, *J. Phys. A* **53**, 355001 (2020).

[20] A. Pal, A. Kundu, and M. R. Evans, Diffusion under time-dependent resetting, *J. Phys. A: Math. Theor.* **49**, 225001 (2016).

[21] V. P. Shkilev, Continuous-time random walk under time-dependent resetting, *Phys. Rev. E* **96**, 012126 (2017).

[22] A. Nagar and S. Gupta, Diffusion with stochastic resetting at power-law times, *Phys. Rev. E* **93**, 060102(R) (2016).

[23] T. Rotbart, S. Reuveni, and M. Urbakh, Michaelis-Menten reaction scheme as a unified approach towards the optimal restart problem, *Phys. Rev. E* **92**, 060101 (2015).

[24] S. Reuveni, Optimal Stochastic Restart Renders Fluctuations in First Passage Times Universal, *Phys. Rev. Lett.* **116**, 170601 (2016).

[25] A. Pal and S. Reuveni, First Passage Under Restart, *Phys. Rev. Lett.* **118**, 030603 (2017).

[26] S. Belan, Restart Could Optimize the Probability of Success in a Bernouilli Trial, *Phys. Rev. Lett.* **120**, 080601 (2018).

[27] A. Chechkin and I. M. Sokolov, Random Search with Resetting: A Unified Renewal Approach, *Phys. Rev. Lett.* **121**, 050601 (2018).

[28] A. Pal, L. Kusmierz, and S. Reuveni, Home-range search provides advantage under high uncertainty, [arXiv:1906.06987](https://arxiv.org/abs/1906.06987) (2020).

[29] P. C. Bressloff, Search processes with stochastic resetting and multiple targets, *Phys. Rev. E* **102**, 022115 (2020).

[30] M. S. Rook, M. Lu, and K. S. Kosik, CamKII $\alpha$  3' untranslated regions-directed mRNA translocation in living neurons: Visualization by GFP linkage, *J. Neurosci.* **20**, 6385 (2000).

[31] J. Dynes and O. Steward, Dynamics of bidirectional transport of ARC mRNA in neuronal dendrites, *J. Comp. Neurol.* **500**, 433 (2007).

[32] C. I. Maeder, A. San-Miguel, E. Y. Wu, H. Lu, and K. Shen, *In vivo* neuronwide analysis of synaptic vesicle precursor trafficking, *Traffic* **15**, 273 (2014).

[33] T. A. Sanders, E. Llagostera, and M. Barna, Specialized filopodia direct long-range transport of SHH during vertebrate tissue patterning, *Nature* **497**, 628 (2013).

[34] T. B. Kornberg, Cytosomes and the dispersion of morphogens, *WIREs Dev. Biol.* **3**, 445 (2014).

[35] E. Stanganello, A. I. H. Hagemann, B. Mattes, C. Sinner, D. Meyen, S. Weber, A. Schug, E. Raz, and S. Scholpp, Filopodia-based Wnt transport during vertebrate tissue patterning, *Nat. Commun.* **6**, 5846 (2015).

[36] E. Stanganello and S. Scholpp, Role of cytonemes in Wnt transport, *J. Cell Sci.* **129**, 665 (2016).

[37] J. Newby and P. C. Bressloff, Quasi-steady state reduction of molecular-based models of directed intermittent search, *Bull. Math. Biol.* **72**, 1840 (2010).

[38] P. C. Bressloff and E. Levien, Synaptic Democracy and Active Intracellular Transport in Axons, *Phys. Rev. Lett.* **114**, 168101 (2015).

[39] B. Karamched and P. C. Bressloff, Effects of geometry on reversible vesicular transport, *J. Phys. A* **50**, 055601 (2017).

- [40] P. C. Bressloff and H. Kim, A search-and-capture model of cytoneme-mediated morphogen gradient formation, *Phys. Rev. E* **99**, 052401 (2019).
- [41] N. Kumar, A. Singh, and R. V. Kulkarni, Transcriptional bursting in gene expression: Analytical results for general stochastic models, *PLoS Comput. Biol.* **11**, e1004292 (2015).
- [42] L. Liu, B. R. K. Kashyap, and J. G. C. Templeton, On the GIX/G/Infinity system, *J. Appl. Prob.* **27**, 671 (1990).
- [43] L. Takacs, *Introduction to the Theory of Queues* (Oxford University Press, Oxford, 1962).
- [44] P. C. Bressloff and S. D. Lawley, Diffusion on a tree with stochastically-gated nodes, *J. Phys. A* **49**, 245601 (2016).
- [45] J. D. C. Little, A proof for the queuing formula:  $L = \lambda W$ , *Operat. Res.* **9**, 383 (1961).
- [46] M. Dogterom and S. Leibler, Physical Aspects of the Growth and Regulation of Microtubule Structures, *Phys. Rev. Lett.* **70**, 1347 (1993).
- [47] H. C. Berg, *E. Coli in Motion* (Springer, New York, 2004).
- [48] D. J. Bicout, Green's functions and first passage time distributions for dynamic instability of microtubules, *Phys. Rev. E* **56**, 6656 (1997).
- [49] D. Campos, E. Abad, V. Mendez, S. B. Yuste, and K. Lindenberg, Optimal search strategies of space-time coupled random walkers with finite lifetimes, *Phys. Rev. E* **91**, 052115 (2015).